5-29-2015

Charging and discharging of Lichtenberg electrets

Monika Wood

Charging and Discharging of Lichtenberg Electrets

by

Monika Wood

Thesis

Submitted to the Department of Physics and Astronomy

Eastern Michigan University

in partial fulfillment of the requirements

for the degree of

MASTERS OF SCIENCE

in

Physics

Thesis Committee:

Patrick Koehn, Ph.D.

James Sheerin, Ph.D.

Ernest Behringer, Ph.D.

Marshall Thomsen, Ph.D.

May 29, 2015

Ypsilanti, Michigan

Acknowledgements

I would like to express my sincere gratitude to my advisor Dr. Patrick Koehn for the continued support of my master's degree and research, for his patience, motivation, and enthusiasm. Thank you for encouraging my research and giving me the confidence to finish. One simply could not wish for a better or friendlier supervisor. I would also like to thank my thesis committee — Dr. James Sheerin, Dr. Ernest Behringer, and Dr. Marshall Thomsen — for their reinforcement, insightful comments, and hard questions. I would especially like to thank Warren Smith, from the University of Michigan Physics Demonstration Lab, for enlightening me to the research topic presented in this paper and for providing me with an excellent atmosphere for doing research. He supplied encouragement, support, and suggestions that fueled the pursuit of this topic. Thank you for assistance in taking photographs and constructing schematics that were used in this paper, as well as his pain-staking effort in proofreading the drafts. My research would not have been possible without his help. Thank you to my fellow co-worker at the University of Michigan Physics Demonstration Lab, Matthew Jackson, for engaging in stimulating discussions that assisted in the development of some of my conclusions. Finally, I would like to thank my family. For my husband Jason Wood who stood by me through this long journey and supported me through good times and bad, for my younger brothers Brett Keith and Alexander Ouimet for pushing me to keep going, and my parents James Keith and Tina Ouimet for believing in me.

Abstract

The research presented here describes a unique way to deposit a large amount of charge onto the surface of a thin dielectric sheet to create a Lichtenberg electret that can be discharged elsewhere to form spectacular Lichtenberg figures. This study examines how the amount of charge deposited onto the surface, the geometry of the probes, and the type of material used can all impact the formation of the Lichtenberg figures. Photographs of the Lichtenberg figures were taken and used to determine the voltage, current, and energy released during each discharge. It was found that a single discharge can release 0.49 J of energy in 1.24 μs for a Lichtenberg figure that covers approximately 500 cm^2. Lichtenberg figures can be used to characterize high-voltage surges on power lines, to diagnose lightning strike victims, to analyze electrical breakdown of insulating materials, for artistic purposes, and for similar applications where pulsed capacitors are commonly used.

Table of Contents

List of Tables

List of Figures

Figures **Page**

Figures **Page**

Introduction

Sparks of electricity may form from one object to another when the electric field between them is large enough to ionize the surrounding environment and allow for the creation of a conductive channel. The abrupt flow of electricity overstresses the atmosphere causing molecules to split and recombine, releasing heat and a flash of light. In the situation where the stored static electric charge on the surface of a dielectric has reached a saturation point and/or is physically perturbed, a distinctive electrical discharge pattern is produced. This paper describes a unique way to deposit and store millions of electron-volts of electric potential energy on the surface of a thin sheet of dielectric in a semi-permanent fashion, and when discharged, a Lichtenberg figure pattern forms like the one shown in Figure 1.

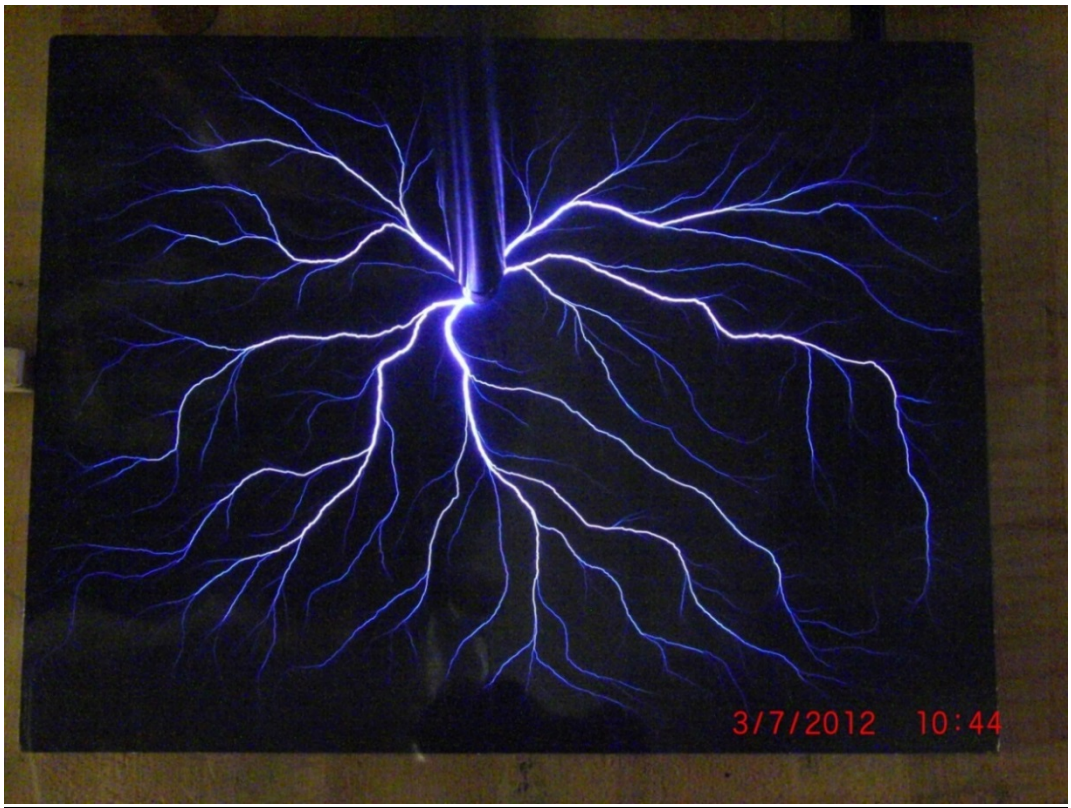

Figure 1: Lichtenberg electret discharge. The size of black image plate is 27.31 cm x 24.13 cm and the sheet was charged for 5 sec/side and discharged with a 0.5 cm diameter discharge probe.

A dielectric is a type of non-conducting electrical insulator that is polarizable when placed in an electric field. The polarization occurs when its molecules gain electric dipole moments that are induced over a certain unit of volume by an external field, known as the polarization density, as seen in Figure 2. Each type of dielectric has a constant with which it describes the relative permittivity of the material, known simply as the dielectric constant, and it is directly related to the electric susceptibility. These characteristics help to restrict the flow of charge along the surface of dielectric materials allowing for the buildup and storage of charge that is deposited onto it.

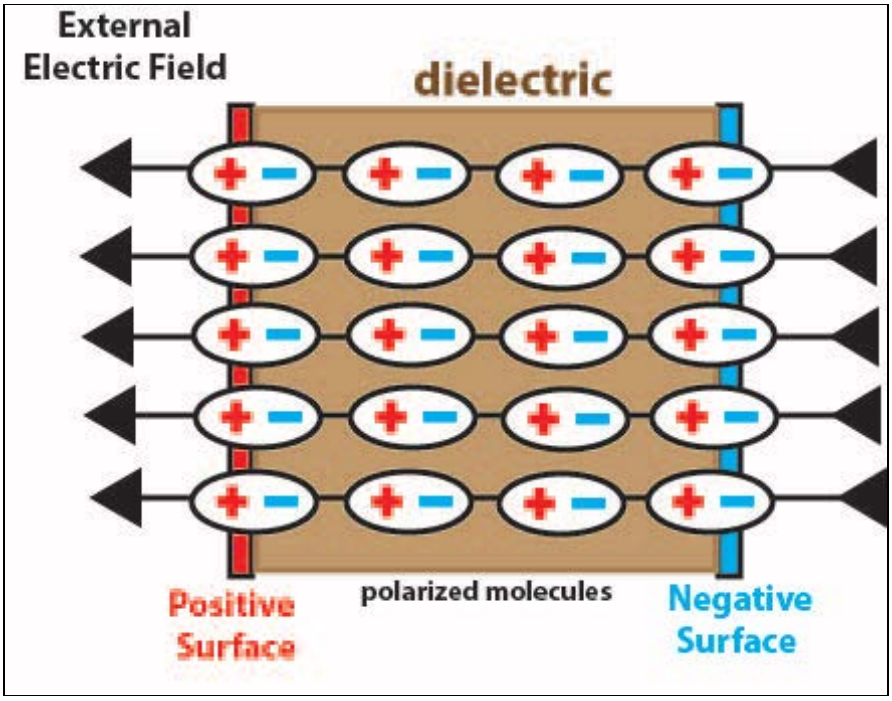

Figure 2: Diagram of a polarized dielectric material placed within an external electric field (Reed).

An electret is the electrostatic equivalent of a magnet and consists of a semi-permanent electric charge embedded upon or within a dielectric material. In this case, the charge buildup of the dielectric is not dependent upon metal plate electrodes with an

electric field applied, but rather the electric charge is deposited directly onto the surface, or embedded in the bulk dielectric, using coronal charging. This in turn creates a rather strong local electric field due to the creation of a dipole across the dielectric. Upon release of the stored energy using our apparatus, a distinctive Lichtenberg pattern is produced along the surface. Due to these characteristics, this apparatus is referred to as a Lichtenberg electret.

To initially charge our dielectric sheet, we use the properties of coronal charging to create a large voltage potential between the surfaces of the test material. Coronal discharges occur when the electric field strength around a conductor is high enough to form a conductive region, but not high enough to cause an arc to form to a nearby object. These types of discharges generate noise in the radio-frequency range and are audible, so we are able to hear them when the induction coil power supply is running. The type of coronal discharges that are used here are known as dielectric barrier discharges (DBD). When a dielectric is placed between two electrodes that are supplied a high-voltage alternating current input, the negative electrode supplies electrons that are accelerated by the electric field produced between the electrodes and then are collected on that surface of the test material. The build-up of the electrons on the negative side of the dielectric will create a local displacement current that will interact with the molecules on the positive side of the sheet. The molecules on the positive side will become ionized by stripping off electrons from the dielectric surface, and these electrons will continue to flow to the positive terminal, as observed in Figure 3. This leaves an excess of negative charge on one side of the dielectric sheet and positive ions on the opposite side of the sheet.

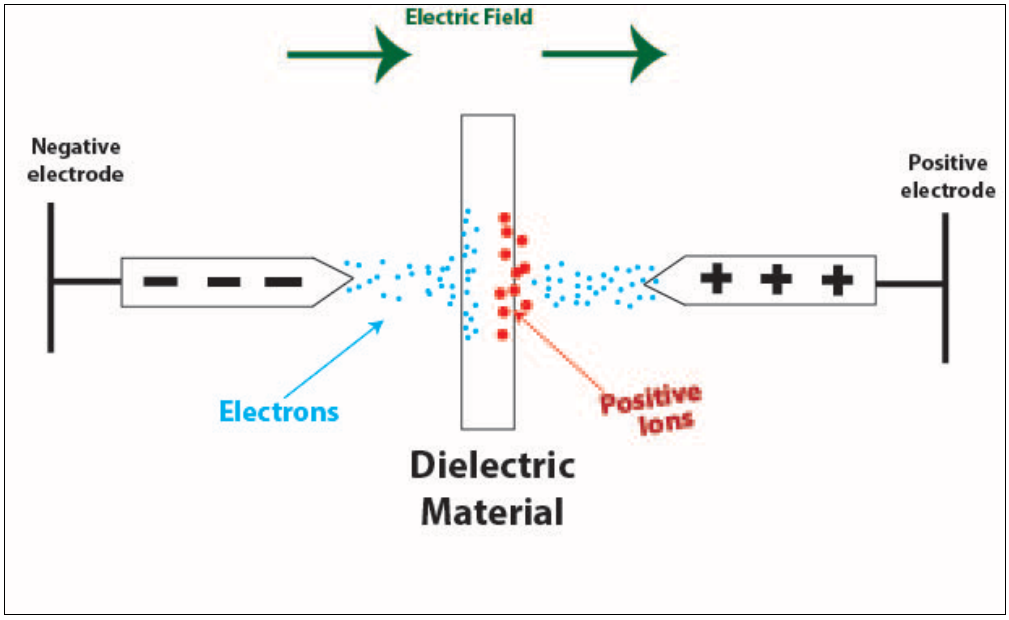

Figure 3: Diagram of the dielectric barrier discharge (DBD) charging method

With a build-up of charge stored on the surface of the dielectric test material, we have essentially created a capacitor. As a discharge probe is brought near the surface of the dielectric, a spark forms. The spark is composed of brush, streamer, and leader discharges. Brush discharges are a type of corona discharge that occurs when there is not enough energy emanating from the electrode and a conductor is not close enough for a spark to form from the electrode to the next closest surface. In the region around the electrode, an accumulation of ions begins to form in the surrounding gas for a certain distance from the tip of the electrode. The size of this region depends upon the geometry of the electrode and the applied voltage.

Streamers are electron avalanches that transfer the charge within the surrounding gas to form areas of excess space charge. A leader electric discharge appears when enough displacement current from enough streamers combine to create a channel of hot plasma. Streamers and leaders are considerably more conductive and hotter than corona discharges. Farther from the initial breakdown point of formation, leader discharges

project the local electric field to allow for the formation of farther streamers. The displacement current of the streamers feed the leaders to help keep them electrically conductive until there are no longer enough streamers to keep the conductivity high enough to create additional leaders. Lichtenberg figures are the recorded images of these branching electrical discharges.

Historical Discovery and Related Literature

Georg Christoph Lichtenberg first discovered Lichtenberg figures in 1777, where he used electrical induction to charge a very large cake of resin, known as an electrophorus, with a large metal plate to collect and transfer the charge (Takahashi 3). At the time of discovery, Lichtenberg's laboratory was under construction and a great deal of dust was in the air. When the potential between the metal plate and electrophorus was high enough, a spark formed from the metal transfer plate to the electrophorus, where it then spread radially along the surface of the resin. On the electrophorus, at the point of the strike, the construction dust adhered to the surface where residual charge lay, exposing a distinctive pattern. The two-dimensional Lichtenberg figures that were revealed became known as dust figures and the method for transferring these to paper became the building blocks for the process known as xerography.

Ultimately, there were two types of dust figures — positive and negative — exposed using two types of electrically charged powders. Positive figures formed where there was positive charge stranded on the surface of the dielectric material. Yellow sulfur becomes electrically negative when agitated, exposing regions where there is residual positive charge on dielectric surface. Red lead (Pb_3O_4) dust, however, becomes positively charged when agitated, revealing negative areas. In an air environment, positive dust figures revealed by the yellow sulfur dust were star-like, developing similar to tree branches as the applied voltage was increased or the gas pressure was decreased (Takahashi 8). Negative figures were generally smaller in size and shaped more like a moon or fan, with no branching taking place within the structure. The distributions of the residual charge due to the discharge or discharge channels remain more or less permanent

on the dielectric material.

Research continued through the 19th and 20th centuries with the development of a procedure to record discharge figures on photographic film. The typical experimental setup consisted of a grounded plate with the dielectric material lying on top of the plate and a photographic plate atop the dielectric, as seen in Figure 4. A needlepoint electrode contacting the dielectric surface is fed an impulse voltage, often using a spark gap to control the input value, to produce discharge patterns emanating from the electrode. This was the basis for a device known as a Klydonograph, which records high-voltage surges on power transmission lines due to lightning strikes (McEachron 718).

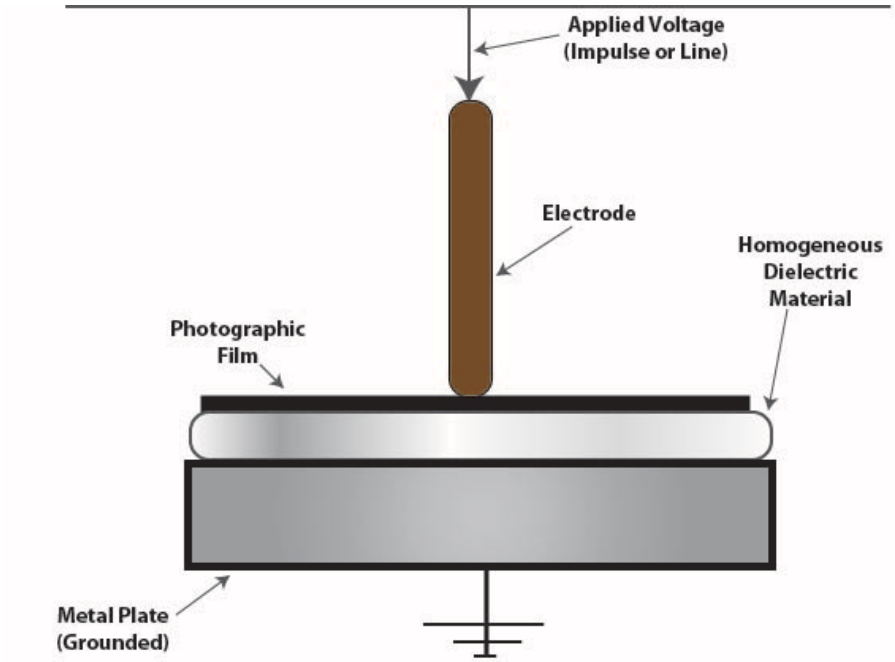

Figure 4: Typical experimental setup used by researchers recording Lichtenberg figures on photographic film

During the mid 1890s, Peter T. Riess discovered that the diameter of positive Lichtenberg figures was about 2.8 times the diameter of an equal-voltage negative figure. In the mid 1920s, Arthur Von Hippel discovered that increasing the applied voltage or reducing the surrounding gas pressure causes the length of the figures to increase

(Stoneridge Engineering). Typical Lichtenberg figures produced were of the size of a few millimeters to a few centimeters in diameter, with the larger figures produced in vacuum environments.

With the creation of pulsed particle accelerators, scientists in the late 1940s began to irradiate blocks of acrylic with electron beams that were powered by high-voltage pulses from a multimillion volt Marx Generator (Stoneridge Engineering). These high-energy beams would embed electrons a certain distance within the block of material, depending on the injection voltage and dielectric properties of the material where the charge would accumulate. To discharge the blocks, an insulated metal tool with a pointed end was used to strike the surface where the charge was collecting. At this point, the electrical stress exceeds the dielectric strength of the material causing the chemical bonds to begin to break and ionize. The electrons become accelerated by the local electric field present within the dielectric, causing an avalanche of electrical breakdown through the volume as the excess charge is released in a beautiful three-dimensional Lichtenberg figure discharge. Since ionization releases both light and heat, the paths of discharge traveling through the acrylic becomes etched into the volume and frozen in time.

More recently, scientists who have placed spacecrafts into orbit have had to combat Lichtenberg figure formation on the surface of thin dielectric materials exposed to the charged solar wind. With constant bombardment of charged particles from the sun, these exposed dielectrics trap the incoming charges on the surface or within the volume. After a period of time, the concentration of charge causes the strength of the electric field to exceed the electrical breakdown of the material. When a discharge occurred, it was found there was substantial physical damage to the sensitive equipment below the

dielectric sheet with evidence that point to a large electromagnetic pulse being produced (Anderson).

Evidence of natural occurrences of Lichtenberg figures can leave a lasting impression on the environment where they form. Lightning strikes are what provide the impulse voltage to the area where figures developed. If a lightning bolt strikes sandy soil, often fulgurites are formed at the site of the strike. Fulgurites are hollow, glass tubes found in sandy soil where the lightning discharge channels heat the sand into glass similar to the paths etched into the blocks of acrylic, as seen in Figure 5. On the surface of grassy fields and pools of water, these tree-like patterns can also form. A photograph of a lightning bolt striking a tree illustrates how the bolt travels through the tree and then spreads out radially across the ground, as seen in Figure 6. Should a person be struck by lightning, the surface of their skin becomes covered in reddish “lightning flowers” as the capillaries are damaged due to the shock wave from the strike traveling along the surface of the skin (Twisted Sifter). An interesting consequence of figures found on humans after a lightning strike is that the patterns will fade as the capillaries are repaired because the damage only occurred on the surface and not deep within the tissue of the skin.

Figure 5: A fulgurite specimen found near Queen Creek, AZ. It is about 14 inches in length with the largest diameter being approximately 2 inches. A cloud-to-ground lightning bolt penetrated the soil and the heat melted the sand grains, then it quickly cooled to a glassy substance (Celestian).

Figure 6: Long exposure of a lightning bolt hitting a tree (ThatScienceGuy).

Since the advent of computer simulations, researchers have been able to mathematically describe the tree-like branching formations that appear in Lichtenberg figures and other natural phenomena (Niemeyer, L., L. Pietronero and H. J. Wiesmann 1035). There is an underlying self-similarity between the full view of a discharge and the sub-structure of the geometry that exists when looking at a highly magnified portion of the discharge pattern. A branch of mathematics called fractal geometry that was developed initially by Benoit Mandelbrot can explain this structure by using a process called diffusion-limited aggregation (DLA), a process where particles undergo Brownian motion and diffusion to drive the mechanism that forms structure (IBM Corporation). When this method of modeling is coupled with an electric field, the mathematical method becomes known as the dielectric breakdown model (DBM), which is the most accurate computer model of Lichtenberg structural formation (Femia, N., L. Niemeyer and V. Tucci 622). Fractal objects do not have integer dimensions, but rather a dimension that falls between two integers. 2-D Lichtenberg figures, for instance, have a fractal dimension between 1.5-1.9 depending on the number of branches that are present in the

image (Stoneridge Engineering).

Lichtenberg figures have a series of distinct characteristics that can be used for practical applications. The Klydonograph was described earlier and has advantages because one can detect both the polarity and magnitude of high-voltage surges on power lines due to lightning strikes. Electricians use Lichtenberg figures to diagnose degradation and electrical breakdown of insulating materials surrounding high-voltage equipment that is inspected. It is also the way that doctors diagnose lightning strike victims. Future research using Lichtenberg figure formation is also quite exciting. Currently, research is being done to use Lichtenberg figure formation within solids as a mold to create artificial biological systems like blood vessels and vascular tissue.

Back in the late 1980s, while working at the University of Michigan, Warren Smith was exploring the dielectric breakdown of various materials. He placed a thin sheet of Mylar between needlepoint discharge probes of a Ruhmkorff induction coil power supply and was burning holes through the thin sheet. When he went to switch hands after irradiating the sheet for a period of time, a large electrical discharge passed through his hand and he observed a flash from the surface of the sheet. Since Mylar is a dielectric, he knew that charge was able to be stored on the sheet, so he experimented with how to charge and discharge these sheets in different orientations.

Initially, he discharged a charged sheet of Mylar with just a wire across the front and back of the sheet producing small sparks. These did not seem as significant as the spark that discharged through his hand, so he tried to place a charged sheet on a plate of aluminum to increase the surface area of the conductor contacting the dielectric. When he discharged the sheet this time, he observed Lichtenberg figures that filled the entire sheet.

This method of discharging became the basis for the way Lichtenberg electrets are discharged in this study. At the time of the discovery, Smith was unable to think of a practical application for this type of discharge and moved on to a different project.

In this paper, two-dimensional Lichtenberg figures are created and studied. The technique of charging dielectric materials described here is unlike the majority of those previously illustrated. This apparatus offers a unique method to deposit charge on the surface of both sides of a thin dielectric sheet using coronal discharges emanating from needlepoint electrodes of a high-voltage induction coil. A digital camera is used to directly image the discharges.

Research Design and Methodology

Producing Lichtenberg figures like the one shown in Figure 1 requires electrostatic charge to be deposited onto both surfaces of a dielectric sheet, separately. For this experiment, letter sized 3M CG3300 Laser Printer transparency film was used as the primary dielectric material studied. During this experiment, there are two main steps to preparing our dielectric. First, the dielectric is charged using a power supply, and then it is placed on a second setup that is used to record the subsequent discharge. For the charging set up, a pair of discharge terminals was connected to the terminals of a high-voltage DC power supply. Initially, an antique Ruhmkorff coil was used, but it was found that more modern solid-state induction coil power supplies also work. Figures 7 and 8 show each type of charging setup, respectively.

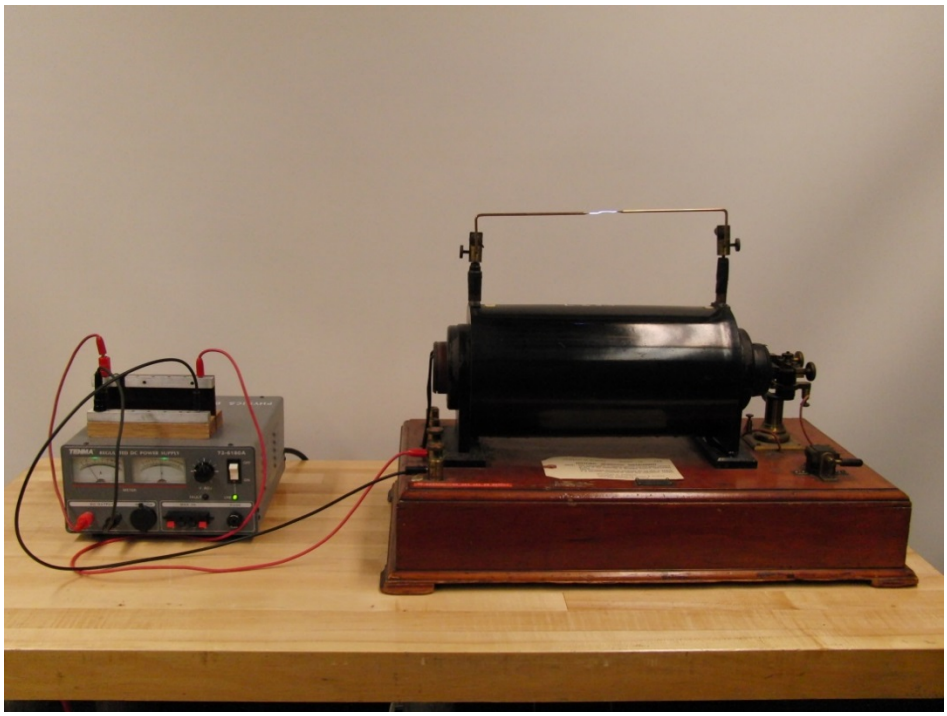

Figure 7: Photograph of the Ruhmkorff induction coil power supply made by Willyoung & Co Philadelphia Maker, circa 1899, charging station. The Ruhmkorff coil is connected to a Tenma 72-6180A Regulated 6 VDC power supply and the output of the coil discharges between the needlepoint electrodes.

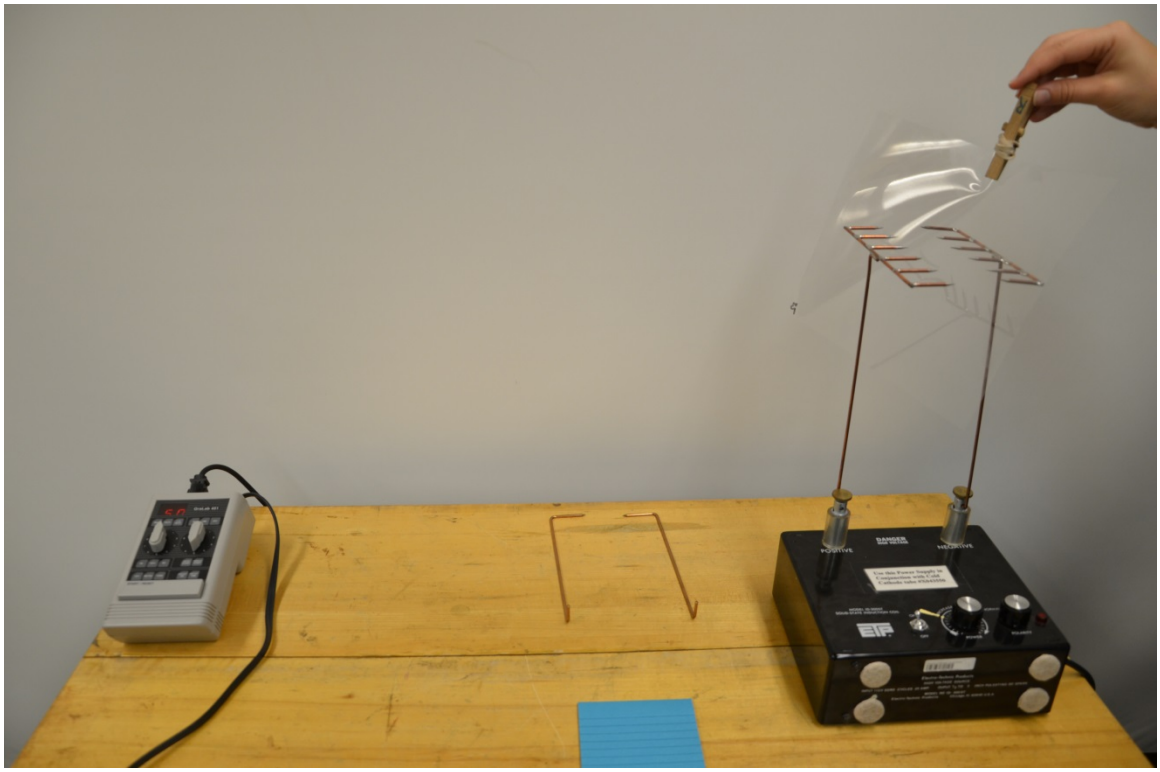

Figure 8: Photograph of the solid-state induction coil power supply, made by Electro-Technic Products Model ID-300ST, charging station. The induction coil has a multi-needlepoint discharge probe attached to each output terminal. It takes 115 V, 50/60 cycle input and converts it into a 3–5 cm pulsating dc spark that is connected to a GraLab Model 451 timer.

An induction coil is a type of electrical transformer that converts a low-voltage input into a high-voltage pulsed output by induction between wire windings with the presence of an interrupter. Each power supply has a primary coil with a few turns of heavy-gauge wire and a secondary coil with miles of fine-gauge wire wrapped around a single iron core. Current passing through the primary coil will create a magnetic field that will be coupled to the secondary coil and enhanced or magnified by the iron core. When current is flowing through the primary coil, the magnetic field created will attract the armature of the interrupter and open the circuit. This break will cause the magnetic field of the primary coil to rapidly collapse and induces a high-voltage pulse in the secondary windings. During this magnetic field collapse, the armature of the interrupter springs

away and closes the contacts to allow the current to flow back into the primary windings, and the process begins again. Due to the large number of windings in the secondary coil, the voltage pulse is typically large enough to produce an electrical spark between the output terminals of the secondary. We placed our test material between these output terminals.

Some experimentation was conducted using a high-voltage Cockroft-Walton dc power supply and a laminated piece of copy paper. This type of power supply is different from the induction power supplies in that it does not use the idea of induction to produce large DC voltages, but rather a type of voltage multiplier. Cockroft-Walton generators convert AC or low-voltage pulsed DC power into higher values of DC power through use of capacitors and diodes. For this type of power supply, the discharge between the output terminals did not produce a coronal spray, but rather a single large electrical discharge, as seen in Figure 9. Since there was no coronal spray, the surface did not have residual charge on it, so we were not able to use our discharge set up. To image the discharge, blue printer toner from inside a broken printer cartridge was used to dust the surface of the laminated sheets and reveal the pattern left behind, as seen in Figure 10. The most interesting part of this image is that the discharge resembles more of a negative Lichtenberg figure, which has a clear perimeter to the discharge figure without much sub-structure within the discharge area. These observations are consistent with those of other researchers (Takahashi 8; Thomas 99).

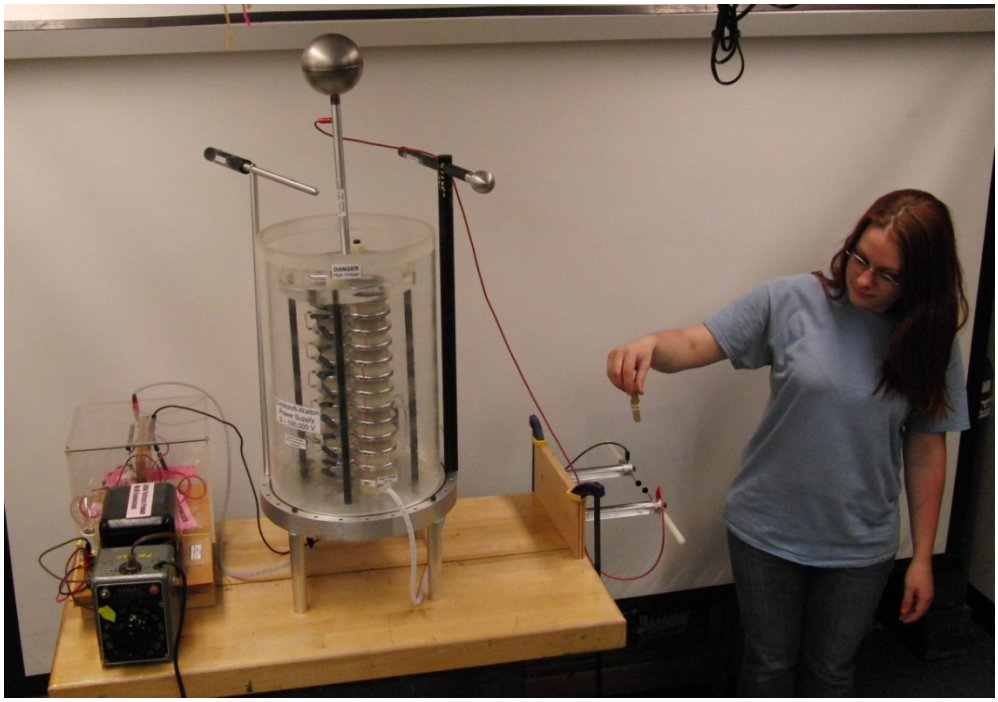

Figure 9: Photograph of the Cockroft-Walton dc power supply setup. The power supply has a pair of probes attached to the output terminals. The voltage multiplier has 10 stages that take the input of 14 kV from the power supply on the left side of the table and ramps the output to over 100 kV. This apparatus discharges in a single pulse, not as a constant stream of ions.

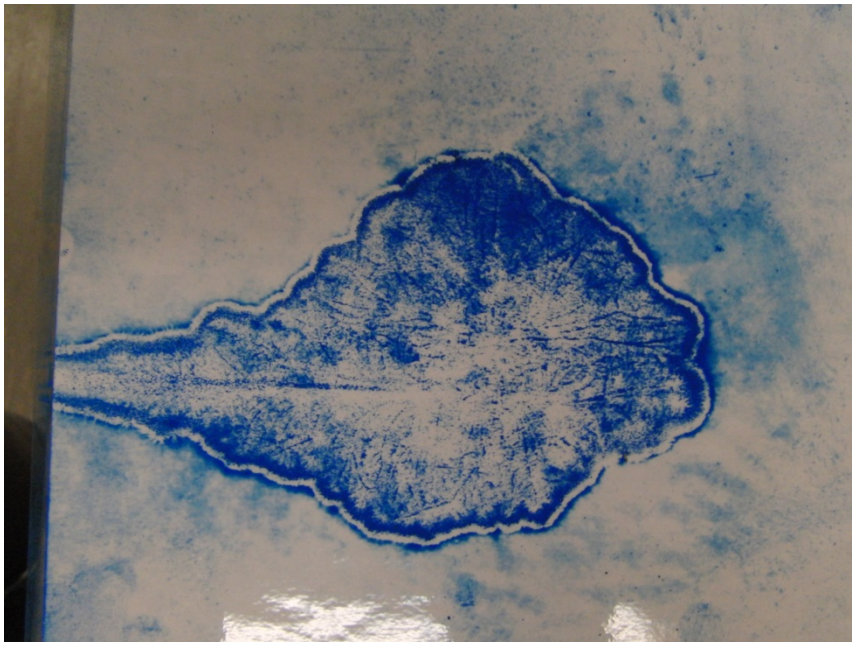

Figure 10: Photograph of a Lichtenberg "dust" figure from the Cockroft-Walton power supply setup. The dust used was from a broken blue toner cartridge from a printer to sprinkle onto the laminated sheet of printer paper after exposed to the discharge from the power supply.

When using the induction power supplies, needlepoint discharge terminals were used to deposit charge on the surface of the test material. Based on the results of the American Institute of Electric Engineers, the relationship between the length of separation of spark gap terminals and the geometry of the electrodes at a given peak spark gap voltage was determined for atmospheric pressure (Weast E-50). It was found that for a given peak voltage, the voltage of the spark produced in the gap between needle point electrodes was larger than the voltage of the spark produced in the gap between any size spherical electrodes. The electric field around an object with a small radius of curvature is much greater than the electric field around an object with a large radius of curvature. The smaller the surface area of the electrode, the larger the coronal spray becomes. Since we are using the coronal spray to deposit the charge onto the test material, we wanted to cover the largest area we could per electrode. During experimentation, the electrodes were typically separated by 3–5 cm, which produced a peak applied voltage from 40-50 kV (Weast E-50). Typically, the area of the test material covered by the coronal spray from a single needlepoint formed a disk with a radius of 3 cm by visual inspection in a dark room.

Initially, a single needlepoint terminal was attached to each lead, but it was found that a multi-point array deposited more charge in less time. The discharge terminal separation of 3–5 cm produced a voltage difference from one side of the sheet to the other that was generally under the breakdown voltage of the dielectric materials studied. If the terminals are set too far apart for the given material, then the electric field strength is above the dielectric strength and the coronal spray can break through the material, causing it to become electrically conductive. This causes partial, but significant, spark

discharges across the surface of the dielectric and the damage decreases the overall storage capacity of the sheet due to the additional edge effects around the newly created holes in the material.

To produce comparably sized Lichtenberg figures to those reported in this paper a particular method of charging of the desired discharge area is required. Insulated pincers are used to handle all charged dielectrics, with care taken to hold the pincers in one hand only, preferably the right hand. A charged Lichtenberg electret, which has no wires or electrodes, should be handled with the same safety precautions as those followed when operating high-voltage capacitors. A modified clothespin with a wooden dowel inserted for the pivot and a rubber band substituted for the metal spring was used to move the charged transparency sheets during each stage.

Charging begins with one side of the dielectric sheet contacting one needlepoint discharge terminal (single or multi-point array), and then the power supply is turned on for a given amount of time. The sheet is slowly rubbed along the positive terminal until the corona discharge spray covered the desired area as shown in Figure 11. Once the positive charge cycle is completed, the opposite side of the dielectric sheet is moved to make contact with the negative terminal of the induction coil. As with the positive side, the negative side of the sheet is rubbed along the negative terminal over the total discharge area. When sweeping across the surface in direct contact with the terminal and charging the second side, it is important for the terminal to stay approximately 1” away from the edges of the dielectric sheet. If this is not done, sparks will snake around and produce partial discharges along the opposite side of the sheet, which again decreases the overall stored charge. Additional alternating charging cycles can be performed to deposit

more charge onto the dielectric surface within the dielectric strength of that material. The duration of the charging cycles were varied, but a common charging time was five seconds per side for a total of ten seconds of charging time.

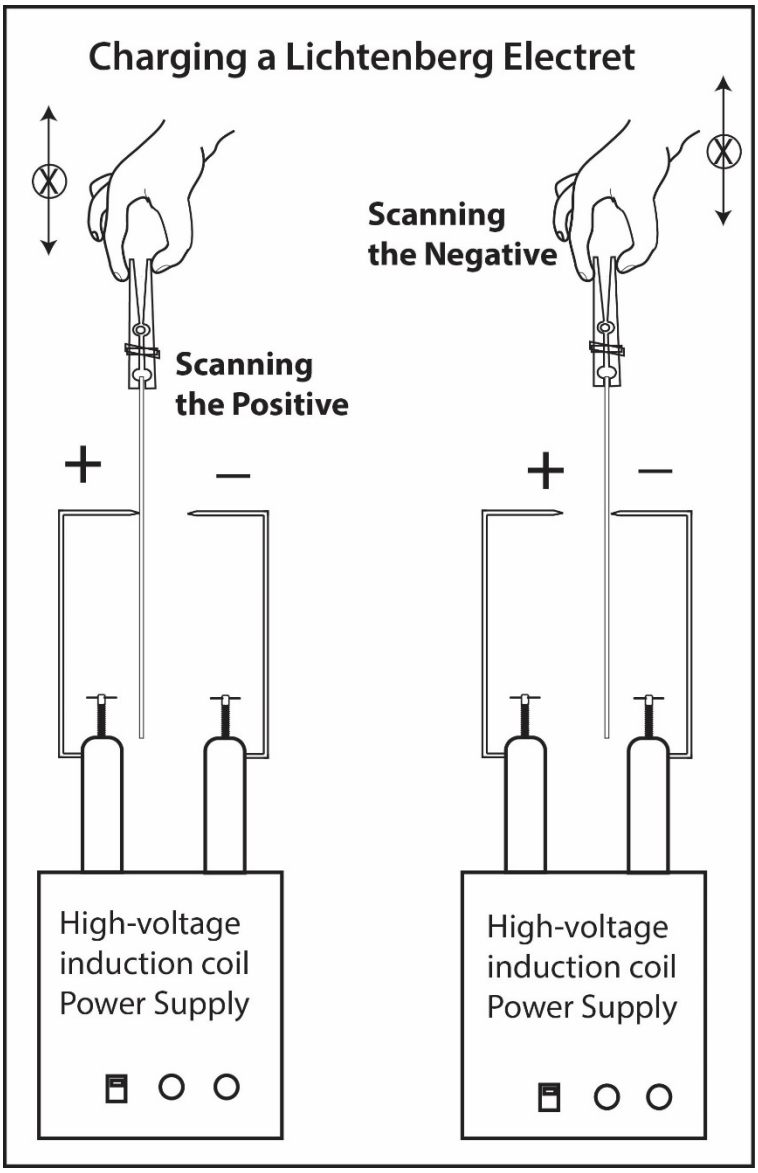

Figure 11: Schematic of the proper way to charge the Lichtenberg electret. The entire surface of the dielectric sheet is scanned by the pulsing DC spark from the high-voltage induction coil power supply (Smith, "Charging a Lichtenberg Electret").

With both sides charged, the dielectric sheet is placed on an ungrounded aluminum plate. Attached to the aluminum plate is an insulated discharge probe with a

wire connecting the two together, as shown in Figure 12. The discharge probe is brought within the vicinity of the top surface of the dielectric sheet until the voltage difference between them exceeds the dielectric breakdown voltage. At this point, ionization of the surrounding air molecules reduces the resistance creating an electrical conduction path for the stored energy on the surface of the sheet to travel along. Since the radius of curvature of the discharge probe is much less than that of the flat plane of the dielectric sheet, the same amount of charge occupies a smaller area resulting in a larger charge density. This is the ignition point of the spark as the gas in the air is converted to plasma.

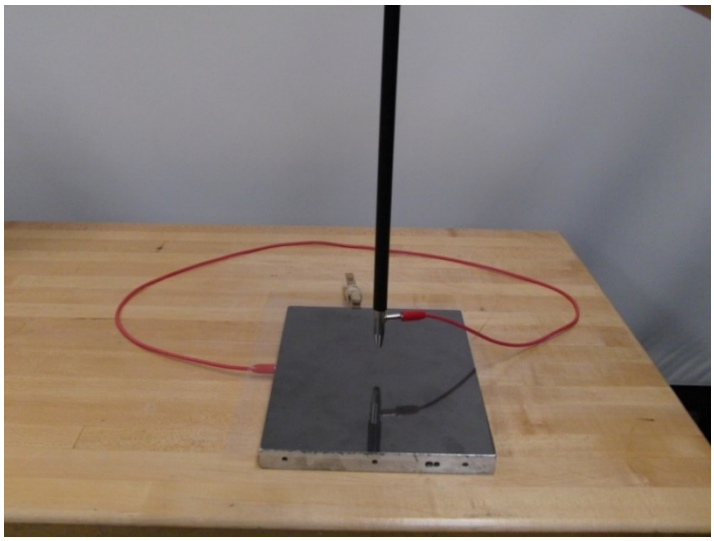

Figure 12: Simple discharge setup with ungrounded aluminum backplane. The charged dielectric sheet is placed on top of the aluminum plate.

Just like lightning in a thunderstorm, the ionization of the air at the surface of the dielectric sheet produces light, sound, and heat. Ionization channels rapidly develop from the probe to the sheet and extending outward along the surface of the dielectric, allowing an electron avalanche to start the flow of current. As more current flows, additional ionization occurs until the local current drops below the holding current. When this occurs, the smaller streamer branches no longer supply enough displacement current to sustain the development of the larger leader branches of the discharge.

To capture the Lichtenberg figures produced during discharge, a digital camera with a timed exposure located in a nearly darkened room was used. Attempts to use high-speed video to capture the figure development proved unfruitful because the discharges occur in approximately 1–2 microseconds and the high-speed camera available could only capture a maximum of 300 frames per second. In order to see the spark evolve, a camera capable of more than 1,000,000 frames per second would be necessary. The best photographs were obtained using a one second exposure time and a sensitivity rating (ISO) set between 400 and 800. A digital camera was placed nearly vertically above the sheet as it lay upon the aluminum plate, with a second camera occasionally used to photograph an edge-on view of a discharge simultaneously.

The value of the current produced during a discharge and how the pulse evolved over time was captured on an oscilloscope. To record this value, a current transformer called a Rogowski coil was placed around the wire that connected the aluminum back plate to the discharge wand and ported that signal through an integrating circuit to the oscilloscope, as seen in Figure 13. A Rogowski coil is simply a helical coil of wire wound on a flexible form that is placed around a current carrying wire to determine the value of the current (Ward, D.A. and J. La T. Exon 106). The current traveling through a wire produces a magnetic field that will induce a voltage in the Rogowski coil, which is proportional to the rate of change of the current through the inductor. The wire connecting the back plate to the discharge rod will induce a current in the Rogowski coil through the creation of a magnetic field, which creates a current in the loops of the Rogowski coil itself. If the coil has *n* turns per meter and a cross-sectional area A that

encircles a current carrying wire with a value of *i*, then any given section of the wire will contain *ndl* number of turns and a magnetic flux given by

$$\Phi = \mu_o \, nA \int B\cos\theta dl \qquad (1)$$

Where the magnetic field has an angular component due to the non-symmetric shape of the flexible coil. This current then induces a voltage in the integrator circuit with an integration time constant of $T = CR_c$, which has a sensitivity equal to the measured current over the measured voltage. For this experiment, a CWT30 Rogowski coil transducer from Power Electronic Measurements Ltd. located in Nottingham, UK was purchased. The commercially constructed integrating circuit of the Rogowski coil had a set scaling factor sensitivity for the oscilloscope output of 1 mV/A with a peak current change of di/dt = 40 kA/μsec.

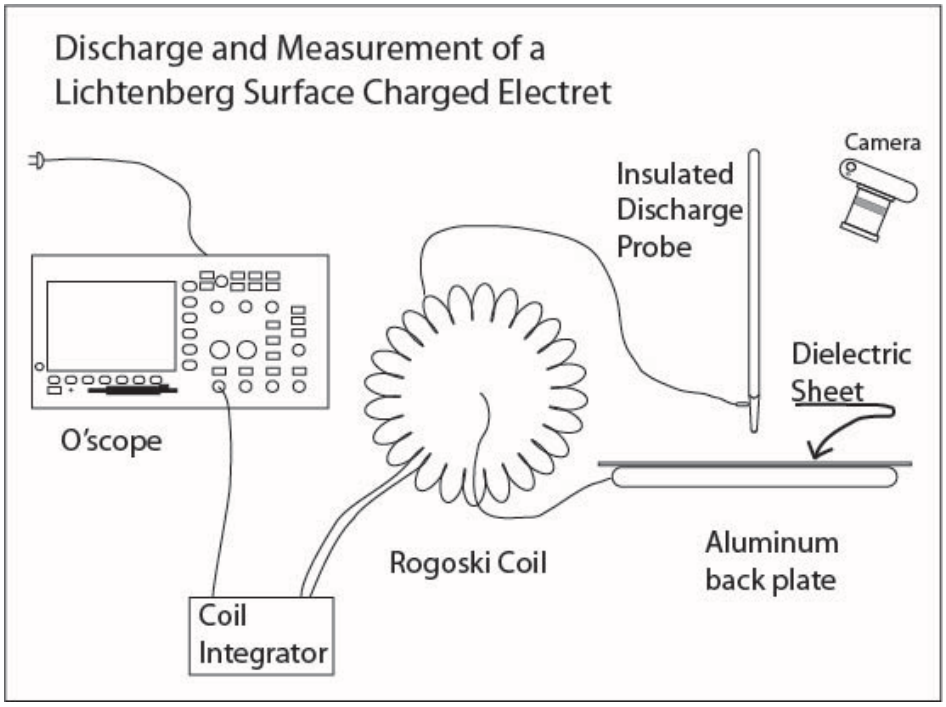

Figure 13: Schematic of the current measurement discharge setup (Smith, "Discharge and Measurement of a Lichtenbergy Surface Charged Electret")

To begin with, a current transformer with a turn ratio of 600:5 made by the Square D Company, catalog number 170R-601, was used to measure the current pulse produced by the discharge, one that contained a ferrite core. Due to the speed of the pulse, the ferrite core introduced induction effects that were difficult to characterize, rendering our data useless. Because a Rogowski coil contains no core, saturation and mutual inductance issues do not occur. In addition to the cleaner and more accurately recorded pulse, the response of a Rogowski coil is linear over a wide range of input values and can be highly customized. It also has a quick response time, which is a necessity when trying to record events that occur in less than a microsecond.

To better characterize how each component of the experimental setup changed the behavior of the electrical discharges produced, different aspects of the basic setup were changed to see how they impacted the formation of Lichtenberg figures. The radius of curvature of the discharge probe that initiates the pulse was varied from a probe with diameter 0.5 cm to one with a diameter of 1.5 cm to a flat circular metal plate. Sheets of charged dielectrics were stacked and discharged in series at different ratios to determine if there are any advantages or correlations to capacitors that are discharged in series. Additionally, different types, surface area, and thickness of dielectric materials were explored to see if all types of dielectric materials are viable and whether the thickness of the material provides any advantages or disadvantages to the storage capacity.

Experimental Data Collection and Analysis

According to the Material Safety Data Sheet provided by 3M, the laser printer transparency film that was used as the primary dielectric material is composed of a Polyethylene Terephthalate (PET) film, which is a form of polyester (Officeworld.com). The typical size of the transparency sheet used was 8.5” x 11” with a surface area of just over 600 cm^2 and a thickness of 0.010 cm. Some experimentation was done on sheets that were 11” x 17” giving twice the surface area with the same thickness of the material. To measure the relative permittivity of the thin film, a small square of it was inserted into a Michelson-Morley interferometer setup and rotated with respect to the optical beam path while observing fringe shifts in the interference pattern (Perger, 4). A schematic of the setup is described in Figure 14. An interferometer works by splitting a single beam into two identical beams, which are then allowed to interfere with each other after they have traveled different path lengths. When two waves of the same magnitude and different phase are superimposed, a fringe pattern of constructive and destructive interference occurs. The interference pattern produced by the interferometer setup used in the study can be seen in Figure 15.

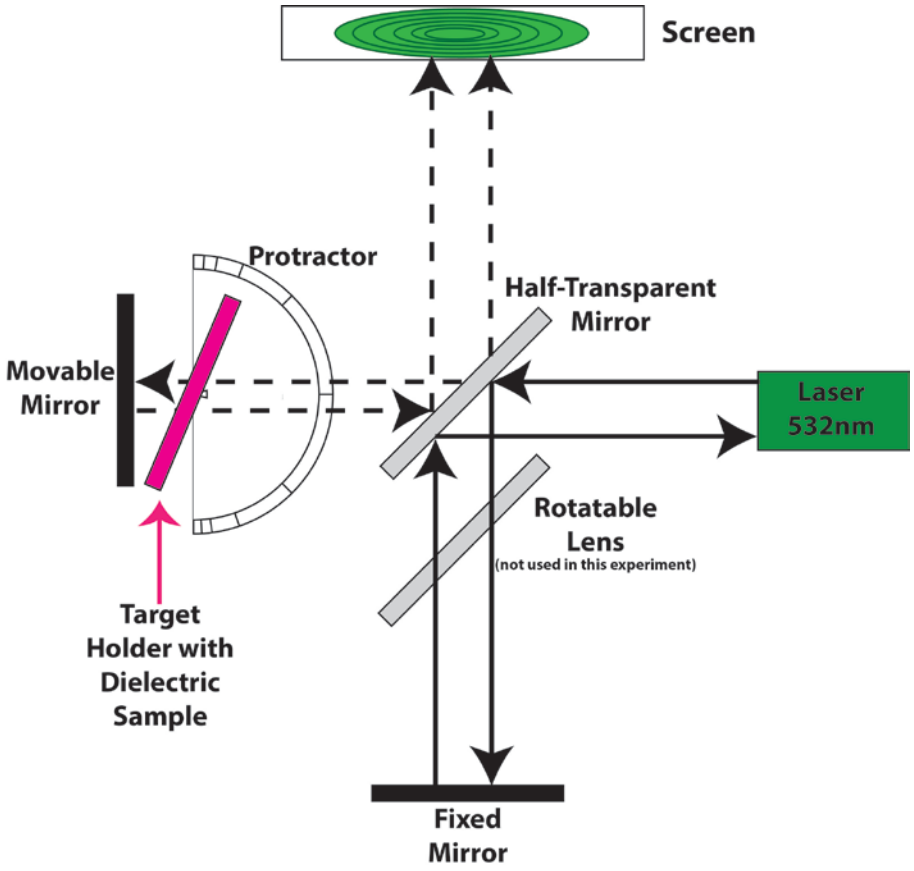

Figure 14: Schematic of the Michelson-Morley interferometer setup. It was used to measure the relative permittivity of the thin film dielectric material studied.

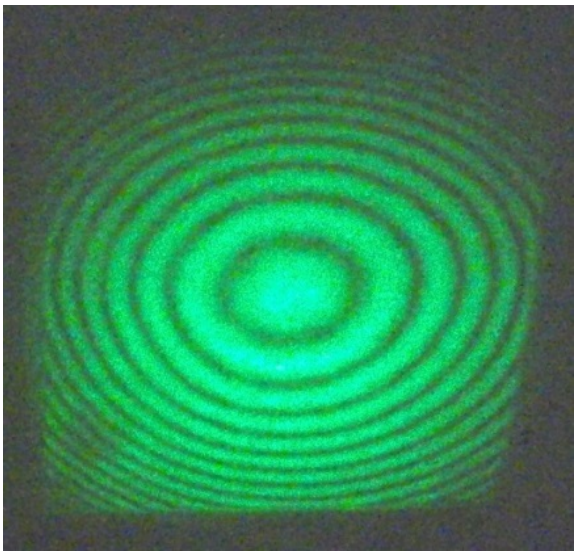

Figure 15: Photograph of the interference pattern produced by the Michelson-Morley interferometer. It was used to measure the relative permittivity of the dielectric material studied.

To determine the relative permittivity of the thin film, the test material was placed in the target holder and oriented perpendicular to the optical beam path. The test material was perpendicular to the optical beam path when small changes of the position of the test holder did not shift the fringes in the image. Then the target holder was rotated slowly as the number of fringe shifts that appeared from the center of the interference pattern was recorded. With the number of fringe shifts known at a given angular displacement, measured using a protractor, the index of refraction can be calculated using the following equation:

$$\eta = \frac{(2T - M\lambda)(1 - cos\theta)}{2T(1 - cos\theta) - M\lambda,} \qquad (2)$$

Where λ is the wavelength of the laser, M is the number of fringes the image shifted, θ is the angular displacement the target holder was rotated, and T is the thickness of the material placed in the test holder. To produce a shift of 20 ± 0.5 fringes, the target holder was rotated 28.0° ± 0.5° relative to the optical beam. If I enter that information along with the wavelength of the laser set at 532 nm and the thickness of the material was 0.0100 cm ± 0.0005 cm, I calculate an index of refraction to be η = 1.74 ± 0.08.

$$\eta = \frac{((2 * 0.00010) - (20 * 532 * 10^{-9}))(1 - \cos(28.0°))}{(2 * 0.00010)(1 - \cos(28.0°)) - (20 * 532 * 10^{-9})} = 1.74 \quad (3)$$

The following relation directly relates the index of refraction to the relative permittivity of a material:

$$\varepsilon = \eta^2 = 1.74^2 = 3.02 \pm 0.30 \qquad (4)$$

Calculating the relative permittivity of the transparency film gives a value of 3.02 ± 0.30, and this result is slightly smaller than the commercially reported value of 3.1–3.5 for this type of material.

Along with the transparency film, there was experimentation performed on copy paper made by the International Paper Company (also known as Hammermill) for use with inkjet or laser printers. This paper is entirely made out of wood pulp and is acid free. Each sheet of paper has the same surface area and thickness as the transparency sheets studied earlier. A sheet of paper was charged the same way as the transparency sheets, and I was unable to produce any kind of discharge with this apparatus. When the paper is placed in the stream of the high-voltage spark, it punctures through and carbonizes the paper. This carbonization creates a circuit connection between the two sides of the sheet and essentially shorts out the corona.

Lexan, a thermoplastic polycarbonate, was available in sheets twice as thick as the available transparency films studied here. According to MatWeb (2011), Lexan has a dielectric constant of 2.8–2.9 which is slightly smaller than the dielectric constant for the transparency film used, meaning it has less capacitance than the transparency film. I was unable to record Lichtenberg discharges of any size on the Lexan sheet with the camera imaging setup. After the Lexan sheet was charged, I could produce small discharges that could be heard, but not seen. Attempts to measure the current released during these discharges were unsuccessful.

Experiments were also done with adhesive tape as the dielectric material. Charging of different types of adhesive tape was interesting because they have a layer of glue on one side of the tape, which is unique to this material. Scotch® brand transparent adhesive tape was first used to combine two sheets of transparency film, side-by-side, together to create a larger surface area as seen in Figure 16. This type of tape is a form of cellulose acetate with acrylate adhesive (American Chemical Society). The two dielectric

sheets were charged in the same way that a single dielectric sheet was charged previously. When discharged, the transparency sheet that the probe interacted with had a Lichtenberg figure discharge pattern appear across its surface, but the discharge pattern did not cross the tape boundary between the two charged sheets as seen on the right in Figure 16. This left the stored charge on the top surface of the second sheet while the stored charge on the top of the first sheet was released during the discharge. Further investigation revealed that the charge on the bottom side of both sheets that was in contact with the non-grounded backplane had been released during the discharge, as expected. Therefore, the transparent adhesive tape was not able to store enough charge to propagate the discharge pattern from one sheet to the next.

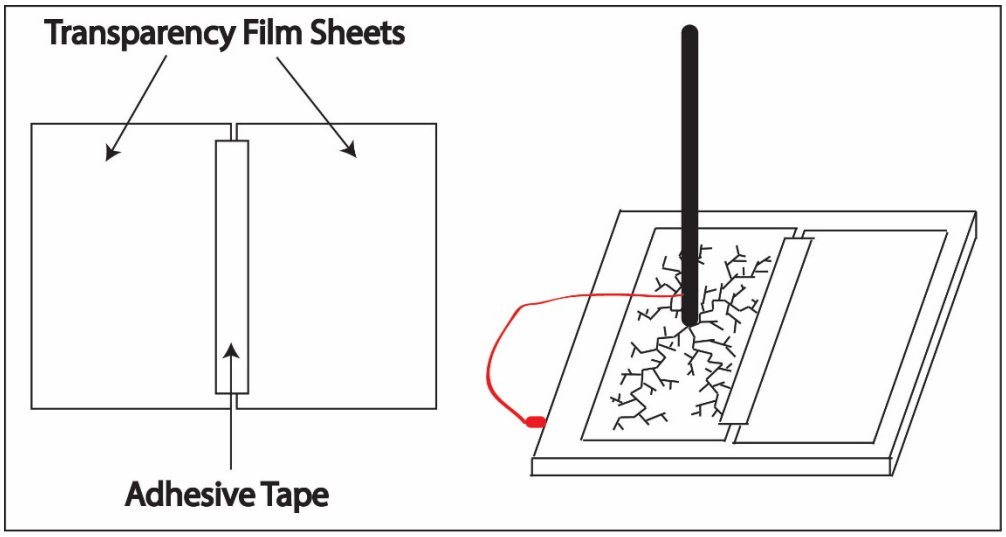

Figure 16: Scotch® brand transparent adhesive tape setup. The right picture is a diagram of a typical discharge pattern observed when in this configuration.

Two types of clear packaging tape were tested, one made of acrylic and another of polypropylene (Scotch 3750; Scotch 311). When a piece of either type of tape was placed between the charging electrodes, small discharge patterns appeared to form in the glue. The dielectric strength of the polypropylene tape is less than that of the transparency film. This was evident when the corona spray created a hole through the tape at an electrode

separation that was below the breakdown value for the transparency sheet. Attempts to produce a Lichtenberg figure on the surface of the tape proved difficult. However, when I folded the acrylic packing tape onto itself, encasing the glue on the inside layer, I was able to store enough charge on the surface to produce small discharges. The acrylic tape had less capacitance than that of the transparency film as I was not able to produce similar sized discharges to those formed on transparency film of the same surface area. Compared to the transparency film, the folded piece of acrylic tape was thicker than the film, which decreased the capacitance between the two sides, as illustrated in Equation 5 where *C* is the capacitance, *A* is the area of the dielectric, and *d* is the thickness of the dielectric.

$$C = {\varepsilon_\circ A}/{d} \tag{5}$$

The majority of the other research on Lichtenberg figures uses a single set up for charging and discharging e.g., Graneau 89; Lee; Mceachron 714; Takahashi 1; Thomas 101; Zeleny 106. Other researchers typically place the given material onto a grounded plate, with one side of the dielectric contacting an electrode of various radii. The initial applied voltage, either positive or negative, is then sent through the contacting electrode. The only charge present on the dielectric resides on the side of the sheet the voltage was applied, and when a discharge occurs, it has the characteristics of that applied voltage. In contrast, the experiment performed here deposits negative charge on one side of a sheet and positive charge builds up on the opposite side of the sheet through the coronal charging method described earlier. Also, a non-grounded backplane is used to rest the charged sheet upon (Thomas 101; Lee).

To confirm that there was indeed a charge separation on each surface of the

dielectric, an electroscope setup like in Figure 17 was used. A known charge was placed on the electroscope using a piezoelectric charger through the attached discharge rod. The charged dielectric sheet was placed on the ungrounded aluminum backplane and the discharge rod that is connected to the electroscope was brought up near the surface of the charged sheet. Since the sign of the charge on the electroscope is known, when the same type of charge resided on the surface of the dielectric, the surface the deflection of the electroscope needle would increase as the probe was brought near. In contrast, when the type of charge on the surface was of the opposite sign, the deflection of the electroscope needle would decrease because the separation of positive and negative charges would decrease. Each side of the sheet was tested, and it was confirmed that there was indeed a charge separation between the two sides of the dielectric.

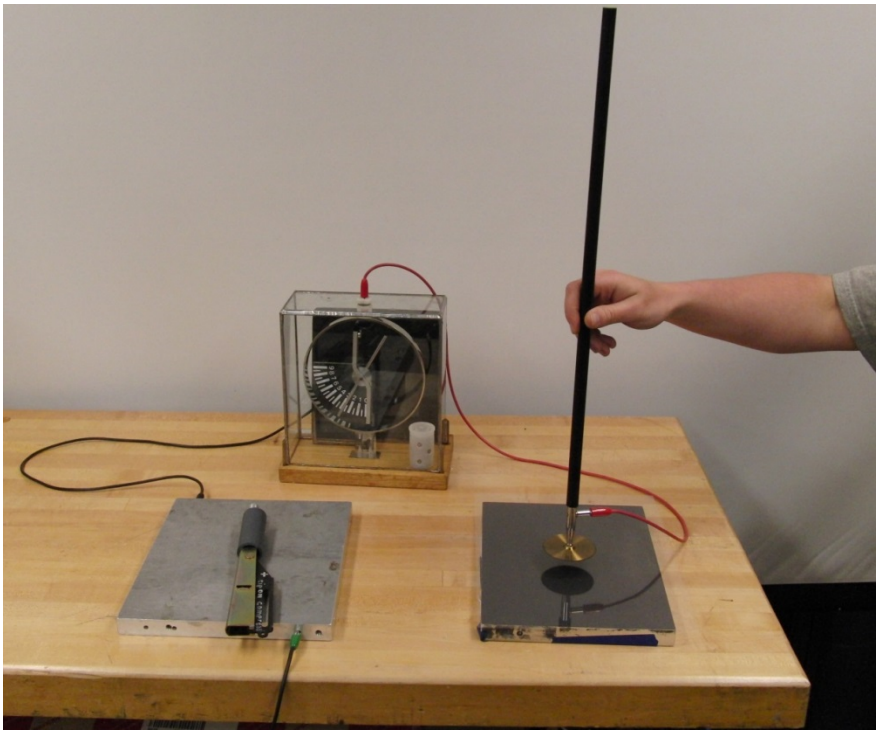

Figure 17: Photograph of sign of charge determination setup using an electroscope and a charged Lichtenberg electret.

With both positive and negative charges present on the surface of the dielectric,

the side of the sheet that is contacting the non-grounded backplane will charge the backplane to the same potential as that side of the sheet. The discharge probe attached to the plane will also have that same potential, as seen in Figure 18. Bringing the discharge probe within the vicinity of the oppositely charged dielectric surface creates a very large potential difference between the two. At the critical distance for the given potential, breakdown occurs with a spark originating at the probe stretching to the sheet and across the surface of the dielectric in less than two microseconds.

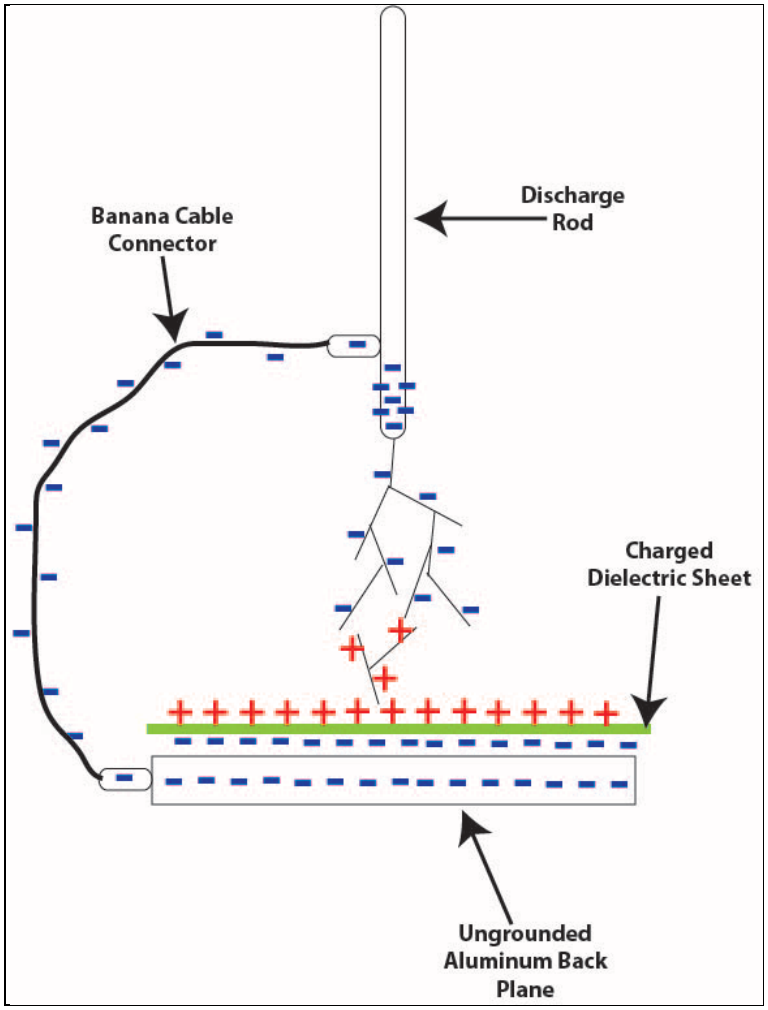

Figure 18: Diagram of the charge distribution and leader discharge formation on a charged dielectric sheet

Research that has been conducted on two-dimensional Lichtenberg figures

discusses the presence of two types of typical discharge patterns observed during experimentation (Graneau 89; Mceachron 714, Takahashi 8; Thomas 100; Zeleny 90). The characteristic discharge patterns are directly related to the impulse voltage applied to the surface of the dielectric through the contacting electrode. During the experimentation conducted here, only positive Lichtenberg figures were produced. This is similar to the figures produced by lightning strikes and the three-dimensional figures produced by particle beam bombardment. In the case of figures produced by these two methods, they both provide large negative applied voltages and produce only positive Lichtenberg figures. As occurs during lightning strikes, the surface of the ground becomes highly positively charged and a channel of ionized air from the negatively charged cloud moves toward the ground. Once there is a completed path between the two oppositely charged regions, the electrical discharge follows. The positive charge is neutralized on the surface, and it races up the plasma channel to the negative regions, where the intense ionization creates the visual spark discharge we can see.

Initially, it was unknown which side of the sheet the Lichtenberg figure appeared. To determine this, a grid was printed onto the surface of one side with black laser printer toner. When the grid was on the underside of the dielectric, the side in contact with the aluminum plate, the Lichtenberg figures were similar in size to those produced on a blank sheet. However, the figures produced when the grid pattern was face up were distorted, as seen in Figure 19. Portions of the major branches often tracked the grid lines rather than traveling in a radial pattern, which makes sense as the ink used to print the grid is made of carbon and polymers that are able to form conduction paths for the deposited charge to travel along with less resistance.

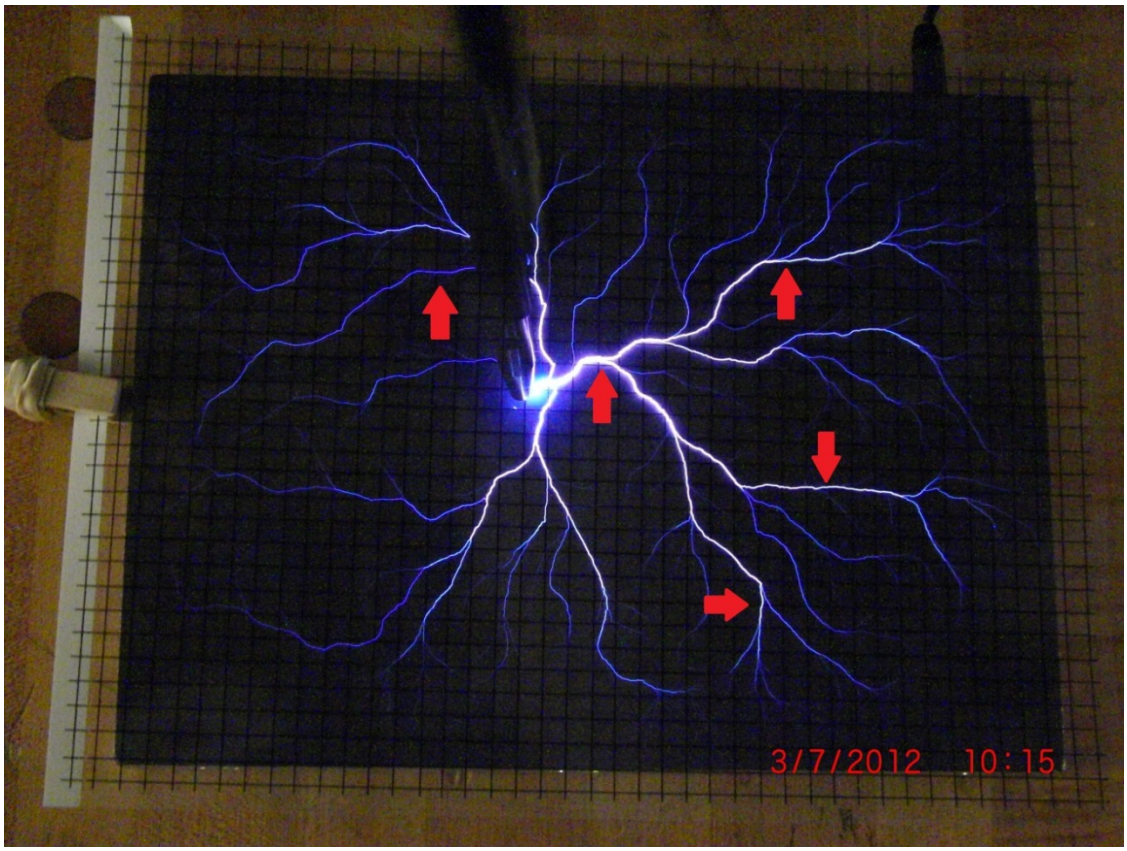

Figure 19: Photograph of a distorted Lichtenberg discharge due to a printed 0.25" grid on the topside of the sheet. This dielectric was charged for 5 sec/side and this picture shows how the gridlines created conduction channels for the discharge to travel along with less resistance, indicated by the red arrows.

Anderson (2012) reported that there is a limit at which the value of the applied voltage will cause the deposited charge to embed into the volume of the dielectric, rather than only residing on the surface. To qualitatively determine if the charges reside on the surface of our sheet, a stream of air was passed across the charged dielectric using a fan. The resulting signal was much weaker than those recorded without the fan running. Anderson (2012) stated that when electrons have energies less than about 100 keV, the charges reside on the surface and deep dielectric charging occurs when energies are greater than 500 keV. With a decrease in the strength of the resulting signal after a fan passed air across the charged dielectric, I would conclude that the energy of most of the

electrons were less than 500 keV and resided primarily on the surface of the dielectric.

To test this statement, a second camera was used to snap a photo of an edge-on view of the Lichtenberg discharge. In the background of the edge-on photographs, a ruler was positioned vertically to give scale. Figure 20 is a photograph taken of a five second per side charging cycle from the edge-on view. It is clearly shown that the discharge occurred before the discharge rod came in contact with the surface of the dielectric as the spark extended approximately 2 cm above the surface of the dielectric sheet. Since each side of the sheet was irradiated for the same length of time, the amount of energy stored on a side are comparable in value. The charge on the top surface of the sheet lies on a flat plane and the charge on the bottom surface of the sheet is connected to the needlepoint discharge probe. When the discharge probe is brought within the vicinity of the top surface of the dielectric, a large voltage difference is present. The charge density along the surface of a flat plane will be smaller than the charge density along a needlepoint due to the radius of curvature of the surface that the overall charge lies along. Since the charge density is larger over the needlepoint and through the discussion of leader discharge formation discussed in Figure 17, this is the likely origin of the discharge. Without a high-speed camera of over 1,000,000 frames per second, the actual evolution of the spark was unable to be studied.

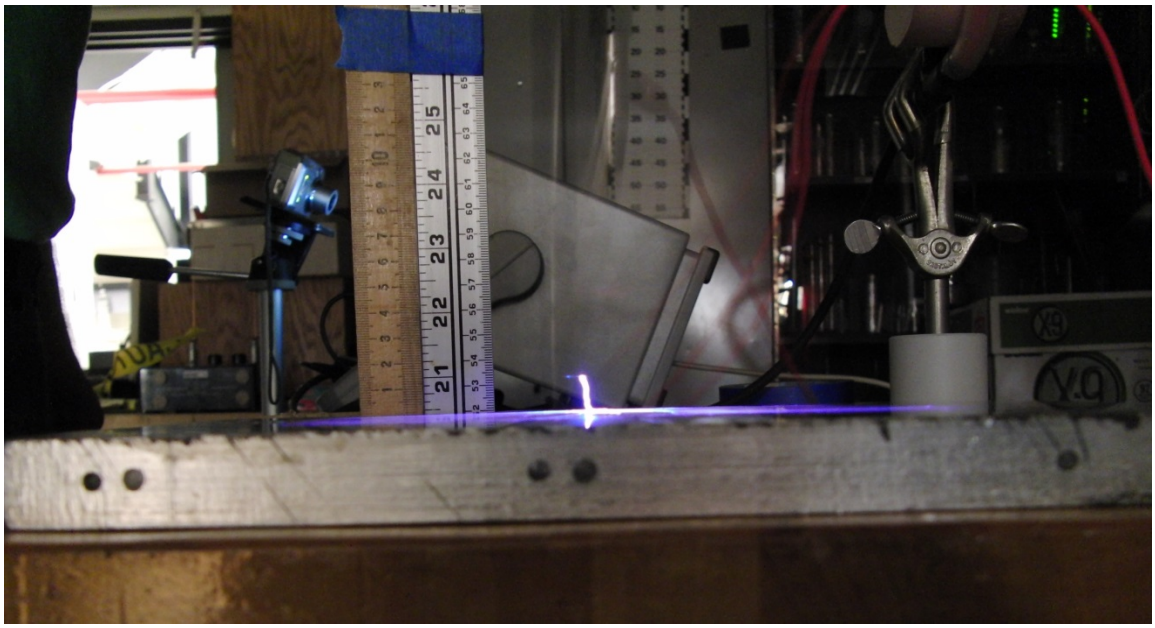

Figure 20: Photograph of an edge-on view of a Lichtenberg figure discharge. It is showing that the spark initiates approximately 2 cm above the surface of the dielectric sheet when the probe is slowly brought towards the charged surface.

The photographs taken, like that in Figure 20, show the spark between the discharge probe and the dielectric sheet initiated before the probe came in contact with the charged surface. The distance above the dielectric sheet where the spark first forms will vary widely depending on how much charge is present on the sheet, how quickly the discharge probe is brought to the sheet manually, how many times a discharge probe was used to initiate a spark, and what type of probe was used to initiate that spark. Variations in the speed of approach of the discharge probe were done at three main speeds that were not precisely controlled, but with some consistency. The slowest approach lowered the discharge probe over many seconds in a slow and methodical decent; while the fastest approach was performed as quickly as possible, and an in-between speed was only used to show a trend from slow to quick. On average, for a sheet charged for a total of 10.0 seconds with a 0.5 cm diameter discharge probe brought up slowly to the surface of the sheet, the spark formed when the probe was about 2 cm above the plate. The faster the

probe was lowered, the closer to the sheet the spark formed when the sheet was charged for the same amount of time.

To explore how the amount of charge deposited by the charging probe impacted the spark pattern produced, the length of time the dielectric was bombarded was varied. Each side of a given sheet was irradiated for 2.0–10.0 seconds per side using a single needle point or multi-point charging probe on each terminal with the high-voltage power supply connected to a digital timer that counted down and turned off when the time expired. When discharged, a photograph of the Lichtenberg figure was taken with a camera and an oscilloscope recorded the current pulse. This method only produced positive Lichtenberg figures due to the way the charge was deposited onto the sheet. Although only positive figures were seen, two variations to the patterns were observed.

The first variation to the discharges observed were those in which the main leader branches extended radially from the origin of the spark and spread outward as the streamers evolved, moving towards the edges of the sheet like the one illustrated in Figure 21. These types of results are typical to results observed by others e.g., Graneau 89; Lee ; Mceachron 715; Stoneridge Engineering; Takahashi 3; Thomas 100; Zeleny 107. In contrast, some discharges produced main leader branches that formed highly curved paths close to the discharge probe like those seen in Figure 22. Curved leader branches were consistently seen when a single sheet was charged for 4 seconds per side, whether that was when each side was irradiated for 4 seconds or when each side was irradiated for 1 second per side for 4 cycles. Both produced at least 1–3 leader branches that followed a curved path closest to the discharge probes. Further from the discharge probe, these paths would then travel in a straight line. Sheets that were charged for less

time always produced radial patterns, and those that were charged for additional time would produce either variation.

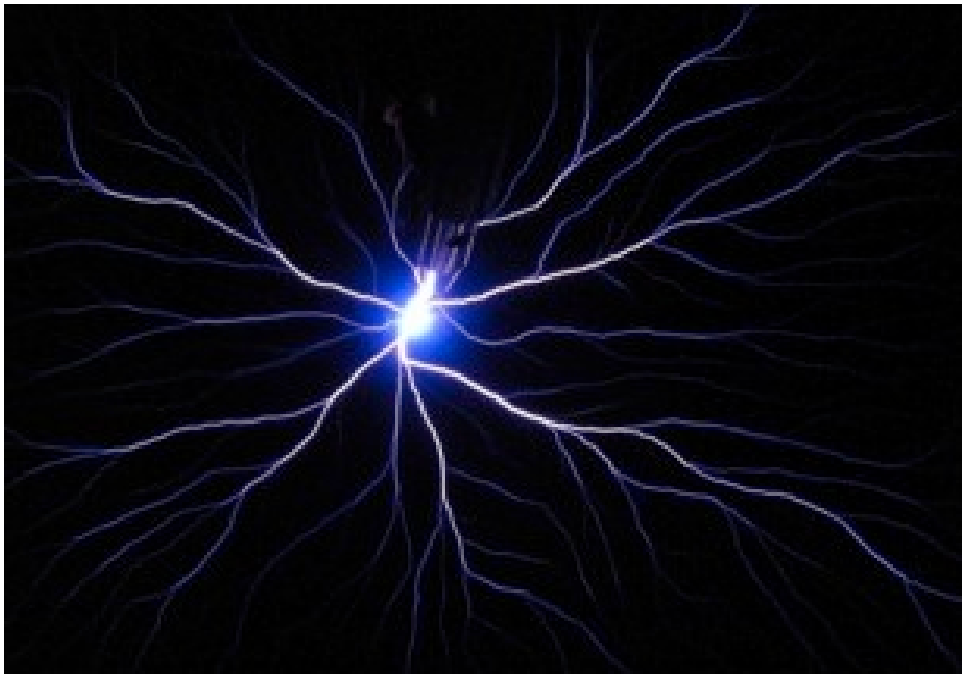

Figure 21: Photograph of a radial Lichtenberg discharge produced by an 8.5” x 11” dielectric sheet that was charged for 3 sec/side.

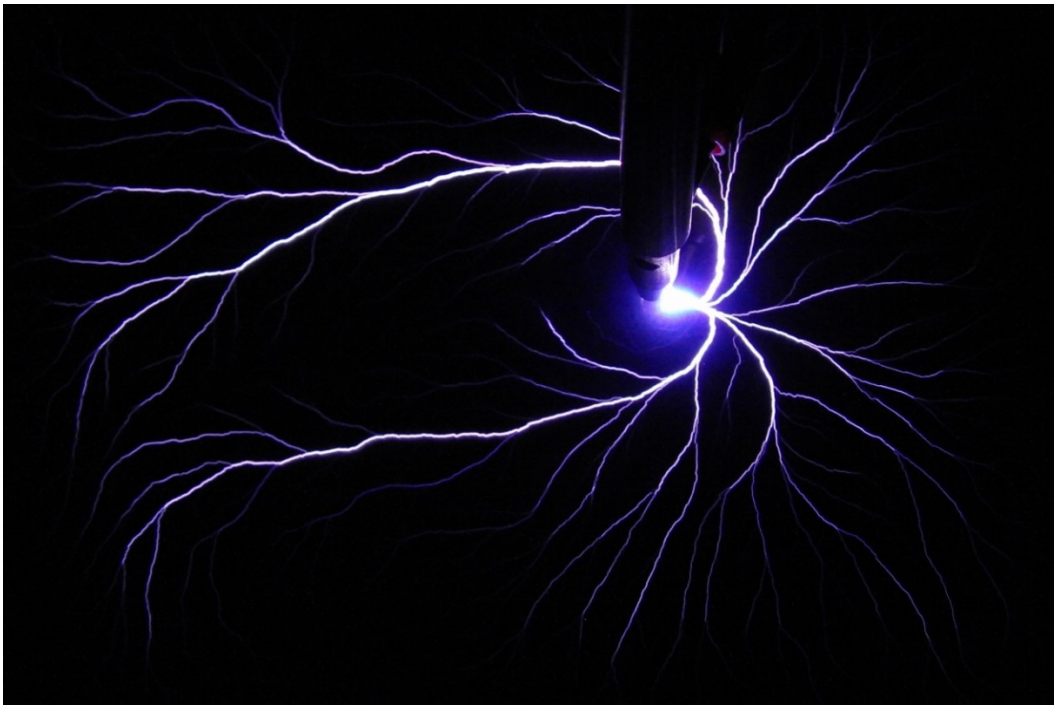

Figure 22: Photograph of a highly curved Lichtenberg discharge produced by an 8.5” x 11” dielectric sheet that was charged for 4 sec/side.

The curving of these leader branches are likely due to the electromagnetic pulse that is produced at the point where the spark has initiated because the current produced here is the sum of all of the possible available current for the rest of the spark. With a flow of current comes the generation of a magnetic field. Since these sparks discharge so rapidly, the magnetic field that is created only lasts for a fraction of that time period. Therefore, the branches closest to the ignition point will experience the effect of the quick production of this magnetic field, but as the branches evolve further from the initial point of ignition, the magnetic field would have already dissipated. As the spark is comprised of charged particles, they experience a force when inside a perpendicular magnetic field causing the particle trajectories to curve in response. Equation 6 describes the relationship between the magnetic field and the applied force where *F* is the magnetic force, q is the particle charge, *v* is the velocity of the particle, and *B* is the magnetic field produced by the spark.

$$\boldsymbol{F} = q\boldsymbol{v} \times \boldsymbol{B} \tag{6}$$

Previous investigators were able to produce Lichtenberg figures that ranged from a few millimeters to a few centimeters in size, except for those produced under vacuum and ones using particle beam bombardment (Graneau 89; Lee ; Mceachron 715; Stoneridge Engineering; Thomas 101; Zeleny 107). The experiments performed here have produced Lichtenberg figures that nearly fill a typical letter sized sheet of dielectric material. Since we were able to fill the entire sheet, we wanted to see if larger figures could be produced on sheets of larger surface area. Therefore, transparency sheets made of the same material and same thickness, but of the size 11” x 17”, were charged using the same charging method. A larger aluminum backplane had to be used, one that had a

size of 11.5” x 17.5”, for our discharge station so that the sheet did not contact other surfaces. When discharged, the Lichtenberg figure produced was even larger than the previously recorded discharges. A photograph of one of the discharges using these larger sheets can be seen in Figure 23, with 18–20 cm sparks radiating from the center of the discharge.

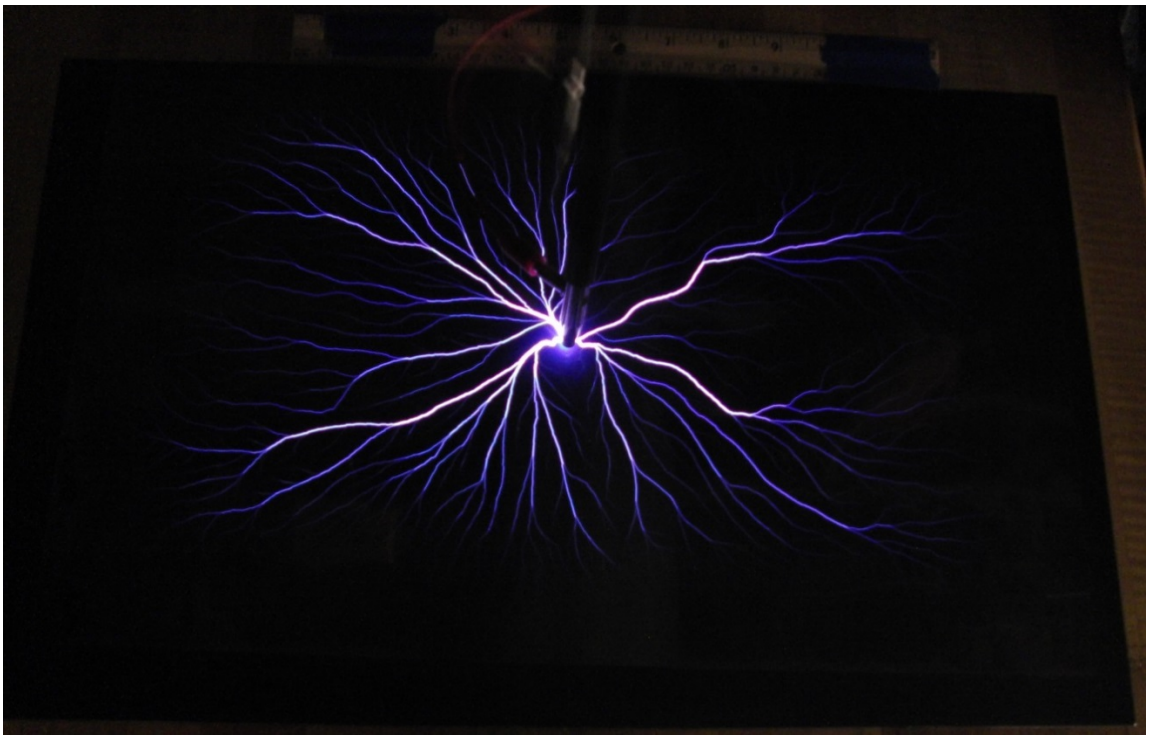

Figure 23: Photograph of a Lichtenberg discharge produced by an 11” x 17” dielectric sheet that was charged for 10 sec/side. The sheet was discharged on a backplane that was 11.5” x 17.5” with a 0.5 cm diameter discharge probe.

With an idea of where the Lichtenberg figure forms and how charging time affects the visual spark produced, numerical characteristics were desired. Voltage measurements of discharge formations are difficult to directly measure. However, the characteristics of spark discharges in air are very well documented. There are two places to estimate the voltage present, one being the applied voltage deposited onto the dielectric sheet and the other is the voltage released by the Lichtenberg formation. The applied

voltage is determined by the separation of the discharge terminals of the induction power supply and the length of time the sheet was irradiated. For this experiment, the terminals were typically separated by 3–5 cm and, as stated before, the peak voltage produced between each needlepoint electrodes was between 40–50 kV.

The maximum power that can be stored on a dielectric sheet from a device that is connected to a wall outlet can be determined. Measuring the voltage input to the induction power supply produced a value of approximately 118 V and the commercially listed input current was 0.25A. The peak voltage output of the power supply was regulated by the separation of the discharge probes to be approximately 40 kV, and the current output from the power supply was measured using the Rogowski coil, as seen in Figure 24, to be 125A ± 5A. Each sheet is irradiated for a total of 4.0–20.0 seconds, so on average each sheet is irradiated for 10.0 ± 0.05 seconds total. The total stored energy present on the sheet after being irradiated by the solid-state induction coil power supply is 50 ± 2.25 MJ, as seen in the calculation below.

$$E = I * V * Time\ Charged = (125A) * (40kV) * (10.0s) = 50 \pm 2.25\ MJ \quad (7)$$

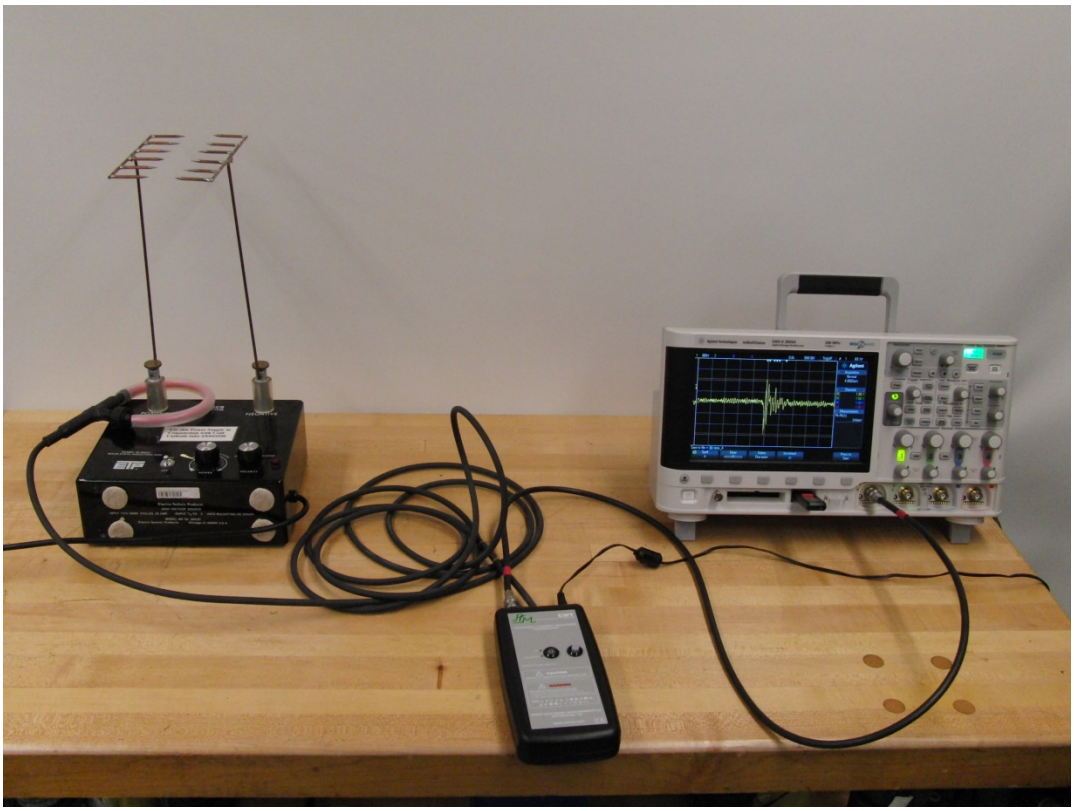

Figure 24: Photograph of the current measurement setup for the output current of the solid-state, high-voltage induction coil power supply used to deposit the charge onto each dielectric sheet.

The sheet is manually moved through the spray stream; therefore, some of the surface is irradiated by overlapping passes and the speed that the sheet was moved through the spray varied because a machine did not perform this step. Since dielectrics resist the flow of electricity, the charge is not able to evenly distribute itself across the surface. This can cause areas to become more densely charged than others, which can contribute to preferential spark formation.

During the formation of Lichtenberg figures, the spark initiates at the tip of a probe and travels through air to reach the surface of the dielectric and then spreads along that surface radially. Characteristics of how a spark behaves in air are used to estimate the voltages we expect to be producing. From the photographs taken of the edge on view of the discharge, the spark formed between 0–2 cm above the surface of the charged sheet

depending on the speed with which the discharge probe was brought to the surface and the potential difference between the plane and the probe. The faster the probe is brought to the surface of the sheet, the faster the rate of change of the potential difference becomes. Graneau (1973) stated that Toepler was able to observe this same relationship between the size of the produced discharge figure and the rate of change of the applied voltage difference.

On average, the Lichtenberg figures produced here had 5–8 main branches that were each 5–15 cm long depending on the applied voltage. According to Zeleny (1945), after a condenser was charged to 9 kV and brought in contact with a dielectric surface for a short period of time, the glass dielectric disk had over 500 Lichtenberg figures under the area covered by the condenser plate, and around the edge of this area was a number of radial lines. He added up the total length of the leader branches of all of the discharges and used the accepted value for the air breakdown voltage to determine how much charge was transferred to the dielectric plate (Zeleny 109). Although the experimental setup was different, the method for determining the released voltage is a viable method to use here since the discharge occurs on the surface of the dielectric material in air at atmospheric pressure. Most often, Lichtenberg figures produced 7 main leader branches that were approximately 8 cm long each. If the total length of the leader branches is calculated and using the average value for the air breakdown voltage as 30 kV/cm is used, then each discharge had a potential of 1.7 million volts.

$$V = L_{branch} * N_{leaders} * V_{air\ breakdown}$$

$$= (8cm) * (7branches) * \left(\frac{30kV}{cm}\right)$$

$$= 1{,}680{,}000\ V = 1.7\ MV \tag{8}$$

To determine the power in a given Lichtenberg discharge, we need the voltage and the amount of current released. As the current flows through the wire of the discharge rod, it produces a magnetic field. Using this principle, the magnetic field of the wire was used to induce a current in the flexible toroidal coil of the Rogowski current transformer that was encircling the wire of the discharge probe. This current then induces a voltage in the integrator circuit of the Rogowski coil with an integration time constant of $T = CR_c$, which has a sensitivity equal to the measured current over the measured voltage.

Before the Rogowski coil was used to measure the current released during a Lichtenberg discharge, a control experiment was done to learn how the current transformer worked. A 10 μF pulsed capacitor was charged to a given voltage and then discharged through the Rogowski coil, where the pulse was integrated and then displayed on an oscilloscope with a scale of 1 mV = 1 A, as seen in Figure 25. The initial charging voltage, the output current value, and the discharge time were recorded for each capacitor discharge and displayed in Table 1 below.

Figure 25: Photograph of the control situation setup to test the Rogowski coil using a 10 µF capacitor.

Initial Applied Voltage (V)	Voltage Recorded by Rogowski Coil (mV)	Peak Current (A)	Average Peak Current (A)	Discharge Time (µs)	Average Discharge Time (µs)
100	16.6	16.6	16.3	9.172	9.116
100	16.0	16.0		9.060	
150	22.1	22.1	22.8	8.795	8.858
150	23.5	23.5		8.920	
200	32.0	32.0	30.0	8.470	8.563
200	28.0	28.0		8.655	
250	37.3	37.3	36.6	8.708	8.785
250	35.8	35.8		8.862	
300	39.6	39.6	44.8	9.090	8.880
300	50.0	50.0		8.670	

Table 1: Testing of the Rogowski coil current transformer on a known pulsed capacitor of 10 µF.

Looking at the data, it is obvious that as the applied voltage is increased, the peak current of the pulse also increases at a rate of about 15 A per 100 V. This linear relationship is what we expect from this device over the applied voltage range. The

discharge time of the pulse was all near an average value of 8.85 μs, showing a rather regular pulse that is put out by this capacitor each time it is discharged. The average power released during the discharge of the capacitor is

$$P = \frac{Q}{t} = \frac{{}^{1}/_{2}\,CV^{2}}{t} = \frac{{}^{1}/_{2}\,(10 * 10^{-6})(200)^{2}}{8.53 * 10^{-6}} = 23.5\ kW \qquad (9)$$

Once the Rogowski coil testing was complete, it was hooked up to the discharge setup for measuring the Lichtenberg figures as shown previously in Figure 13. After a transparency sheet was charged for a given time, between 2.0-10.0 seconds per side, then the sheet was placed on the ungrounded aluminum backplane with attached discharge probe. Each time the sheet was discharged, the Rogowski coil current transformer recorded the pulse. When analyzing the discharge patterns on the dielectric sheet, it is important to note that the charging method used here does not consistently deposit the same amount of charge onto the sheet each time it is irradiated. Looking at the data, it was found that the discharge time of the Lichtenberg pulse remained remarkably consistent even though the amount of charge present was different. Every recorded discharge pulse occurred in less than 1.50 μs. Using the Rogowski coil, the duration of the current pulse could be determined with a resolution of nanoseconds. The results of data collected can be found in Table 2.

Charging Time per side of sheet (s)	Average Discharge Time (μs)	Average Peak Current (A)	Maximum Peak Current (A)
2	1.15	9.68	12.5
3	1.37	12.1	14.9
4	1.10	14.3	16.9
5	1.25	14.4	32.0
6	1.21	13.4	28.0
8	1.27	16.5	20.9

Table 2: Data collected from the recorded Lichtenberg figure discharges using the Rogowski coil current transformer.

Data of a given current discharge was then used to determine an equation for the evolution of current over time. Using the MatlabR2014a curve fitting tool available in the software, the data was loaded and an equation for the current pulse was calculated and displayed in a graph, as seen in Figure 26. To better describe the equation of the curve, the leading brush discharge data was removed from that which was used to calculate the best fit curve. The best fit curve for this type of pulse was a first-order Gaussian distribution with a 98.12% confidence. Below is the equation for the generated best fit Gaussian distribution:

$$I(t) = 30.68\, exp^{-\left(\frac{t+6.186*10^{-7}}{2.860*10^{-7}}\right)^2}\ (Amps) \qquad (10)$$

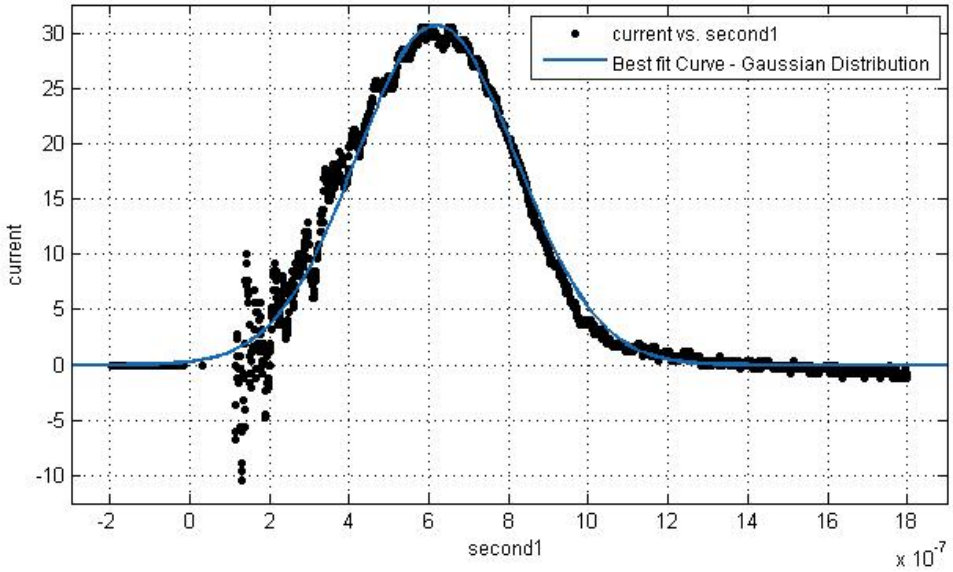

Figure 26: Graph of the current pulse of a Lichtenberg figure discharge generated in MatlabR2014a using data collected with the Rogowski coil current transformer. The brush discharge data was removed, and the best fit first order Gaussian distribution curve is shown in blue.

Given the equation for the evolution of current and using our estimated value for the voltage potential of the Lichtenberg discharge, an equation for the instantaneous power can be calculated:

$$Power = I(t) * V = \left(30.68\, exp^{-\left(\frac{t+6.186*10^{-7}}{2.860*10^{-7}}\right)^2}\right) * (1.7 * 10^6)$$

$$= (5.2 * 10^7) exp^{-\left(\frac{t+6.186*10^{-7}}{2.860*10^{-7}}\right)^2} (Watts)$$

$$= (52) exp^{-\left(\frac{t+6.186*10^{-7}}{2.860*10^{-7}}\right)^2} (MW) \qquad (11)$$

Since power is related to energy, we can also calculate the amount of energy released during a given discharge by integrating the power over the time range of the discharge to give us the area under the power curve, as seen in Equation 12.

$$Energy = \int_{t=t_o}^{t=t_f} P\, dt = \int_{1.14*10^{-7}}^{1.35*10^{-6}} (5.2 * 10^7) exp^{-\left(\frac{t+6.186*10^{-7}}{2.860*10^{-7}}\right)^2} = 0.49\, J \quad (12)$$

The amount of energy released is 0.49 J in 1.24 µs. The rate at which energy was released during a single discharge is about 20 times as large as the power released by the 10 µF pulse capacitor.

Figure 27 is a picture of a typical waveform that is produced when a dielectric sheet is discharged through our Rogowski coil current transformer. There are a few features of the discharge waveform that are worth noting. First, the peak value of the discharge current released was 30 A with pulse duration of 1.24 µs. According to Graneau (1973), the light emitted during the formation of a Lichtenberg figure is the result of electron avalanches proceeding tangentially along the surface of the dielectric material. Prior to the main pulse is a 200 ns long brush discharge, which is what initiates the intense ionization that cascades across the surface of the sheet (Mueller). The speed

with which the discharge probe was brought near the charged sheet will affect the way that the brush discharge evolves. Using a different discharge probe, one with a diameter of 1.5 cm, the brush discharge before the main pulse was much more intense and occurred for twice as long as the brush discharge produced the 0.5 cm diameter discharge probe, as seen in Figure 28.

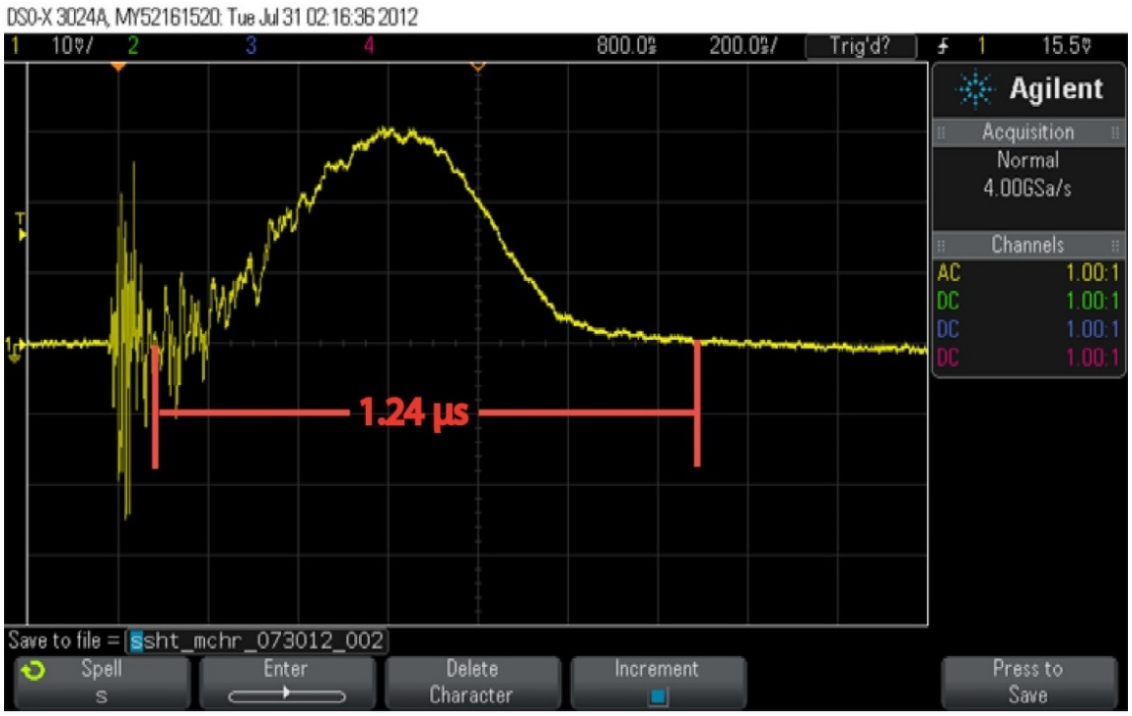

Figure 27: Photograph of the oscilloscope trace capture of a Lichtenberg discharge using a 0.5 cm diameter discharge probe. The peak current was 30 A (scale 1 mV/A) with a 1.24 µs total pulse width (not counting the brush discharge at the leading edge of pulse) of a single sheet charged for 5 sec/side.

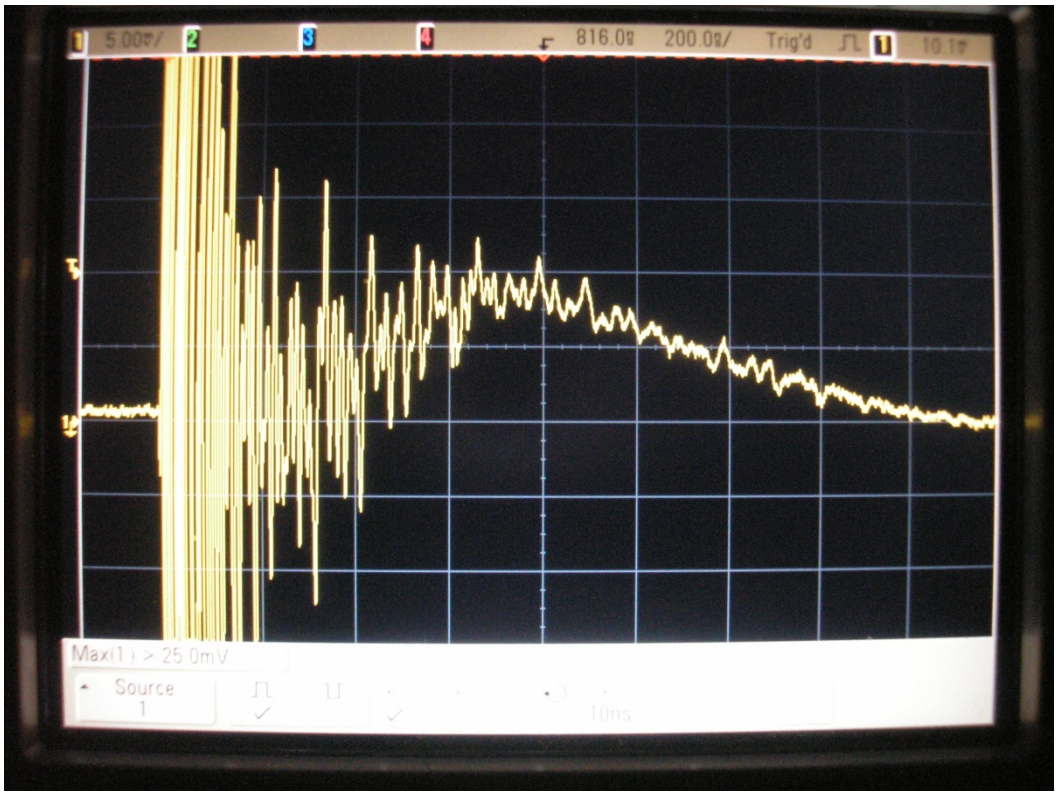

Figure 28: Photograph of the oscilloscope trace capture of a Lichtenberg discharge using a 1.5 cm diameter discharge probe. The peak current was 10.1 A (scale 1 mV/A) pulse with a discharge time of 1.3 µs (not counting the brush discharge at the leading edge of pulse) of a single sheet charged for 5 sec/side.

Further investigation of discharge probe geometry continued with the use of a 17 cm diameter flat metal charge transfer plate with insulated handle and the backplane from the original experiment, creating a setup similar to a parallel plate capacitor. The major difference between a true parallel plate capacitor and the setup described here is that the dielectric material is charged rather than applying a potential difference to the metal plates of the capacitor directly. To discharge the system, the same discharge probe, which was connected to the ungrounded backplane, is brought into contact with the metal charge transfer plate that was placed on top of the charged dielectric sheet that was placed on top of the backplane. Radiating from the edge of the entire circular plate area were a series of discharge branches that range from 5–10 cm long around the entire plate,

as seen in Figure 29.

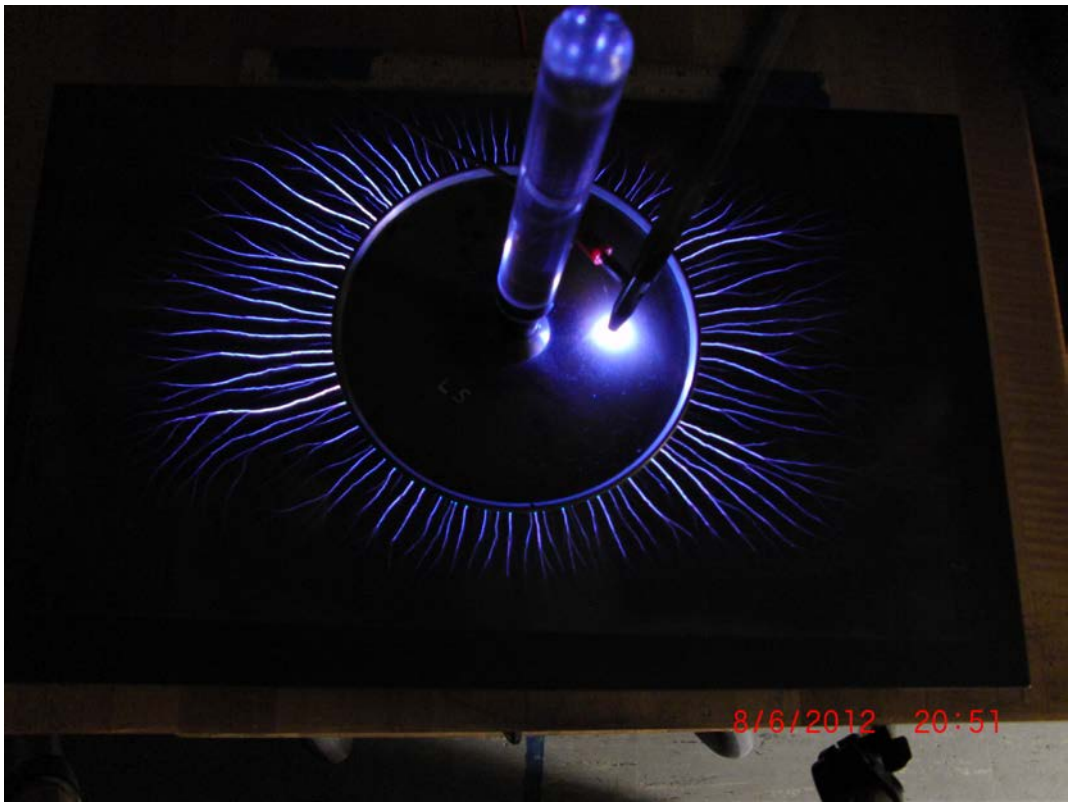

Figure 29: Photograph of an 11” x 17” dielectric sheet discharge from a 17 cm diameter flat, circular metal charge transfer plate.

To estimate the amount of voltage potential of the discharge of the metal plate on a letter sized transparency sheet, we calculated the total length of all of the visible leader branches to be approximately 175 cm. Using Equation 4, the amount of voltage potential of the discharge was at least 5.25 million volts or over three times that present when using a 0.5 cm diameter discharge probe. Recording the current pulse using the Rogowski coil revealed that the peak current released and electric potential energy present when in this configuration was about five times as large as when we discharged the Lichtenberg electret with a single point probe. In addition to the increase in current and voltage released, the waveform of the pulse was of a different shape than previously recorded. Like before, it had the initial brush discharge that leads the main pulse, but after the main

pulse is what seems to be an under-damped oscillation of the current as it comes back to zero, as seen here in Figure 30.

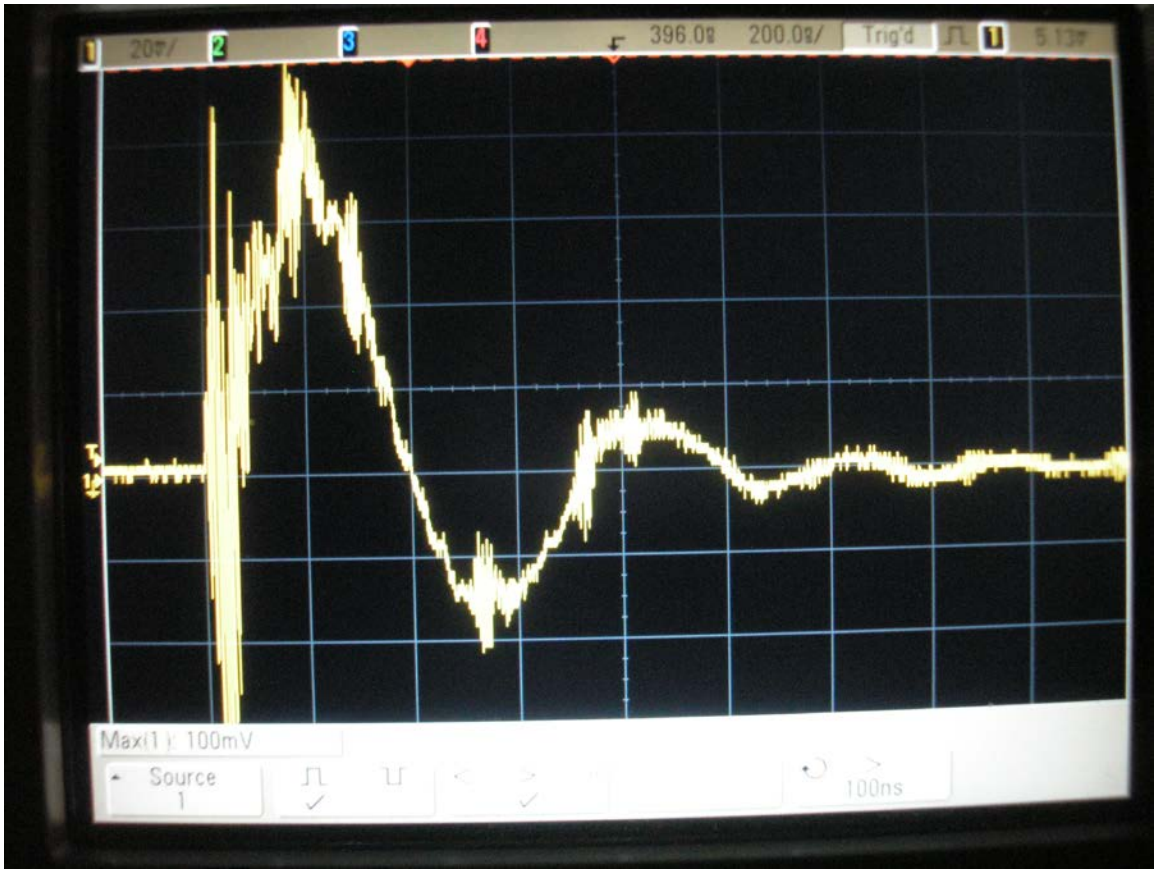

Figure 30: Photograph of the oscilloscope trace capture of a Lichtenberg discharge using a flat plate discharge probe. Observe the different pulse shape with a peak current of 100 A (scale 1 mV/A) for a single sheet charged for 5 sec/side.

Under-damped oscillations are often found in RLC circuits when sudden changes to the steady state of the system, usually with the rapid increase or decrease in voltage, cause a transient response in the circuit as the system tries to reach a new steady state. According to the manufacturers of the Rogowski coil, if the current rating of the transducer is exceeded the integrator will become saturated and the measured waveform becomes corrupt rather than clipped like what is seen when using an amplifier (Power Electronic Measurements Ltd. 13). The time it takes to return to normal operation is

dependent on the low frequency bandwidth of the unit, which is 0.6 Hz for the model Rogowski coil used here. According to the data presented in Figure 30, it takes the Rogowski coil approximately 1.250 μs to recover from saturation. To better characterize the current pulse of Lichtenberg discharge produced by the flat, circular plate a Rogowski coil that is more tuned to the larger peak current pulse must be purchased to get more reliable data before much more can be concluded.

Knowing how much energy can be released by a given charged electret, I wanted to explore whether these sheets could be stacked in series like capacitors to see if they had similar properties. Charged sheets can be carefully stacked on one another and discharged as one large collection in certain stacked configurations. When the sheets were stacked so that every negative side came in contact with the other negative side of the sheet below it and an odd number of sheets were used, like that illustrated in Figure 31 (A), successful discharges of the stack of dielectrics occurred. A photograph of a successful discharge can be seen in Figure 32. The current pulse released by the discharges of these types of stacks generally had a larger peak current as the number of sheets that were stacked increased, but there was no consistent trend to the results. With charge lying in layers between the sheets of dielectric, there may be other mechanisms playing a role in the flow of charge from the bottom of the stack to the top. Peak current values as high as three times that achieved with a single sheet were observed. Recorded current pulse widths decreased as the number of stacked sheets increased, but the waveform shape of the overall current pulse was similar. Stacking the sheets in the opposite orientation, where positive sides are contact negatively charged sides like that illustrated in Figure 31 (B) and (C), caused the sheets to neutralize most of the stored

surface charge. The residual charge left after neutralization was on the same order as that stored on a single dielectric sheet, but now the two charged surfaces were separated by a larger distance. This decreased the overall capacitance of the system, resulting in the lack of recordable Lichtenberg discharges.

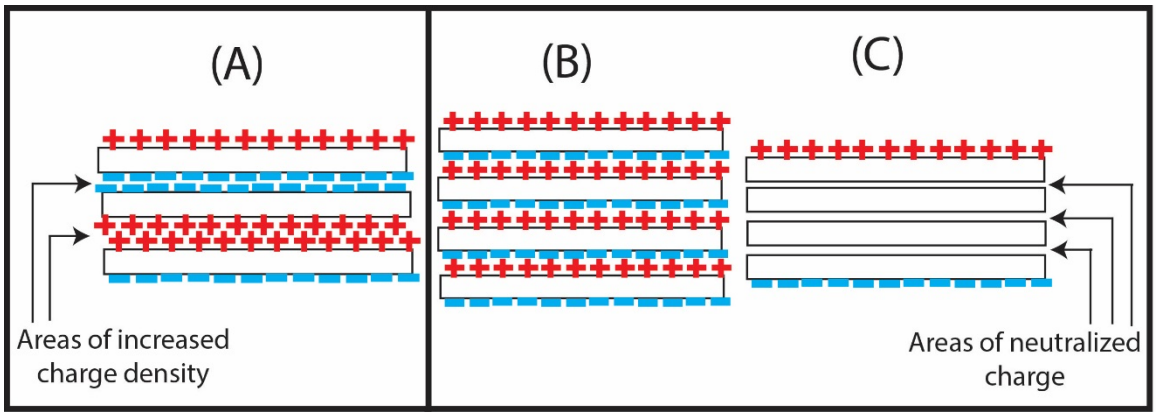

Figure 31: Diagram of charged dielectric sheets carefully stacked on one another prior to discharge. (A) When stacked with like charged sides in contact with each other and an odd number of sheets used, successful discharges occurred. (B) When stacked with oppositely charged sides in contact with each other and an even number of sheets used. (C) Resulting charge neutralization of the oppositely charged contacting surfaces of the stacked sheets leaving similar stored charge on the outer surfaces as a single sheet. Due to further separation between the two charged sides of the top and bottom sheets, the capacitance is reduced and no discharges were recorded.

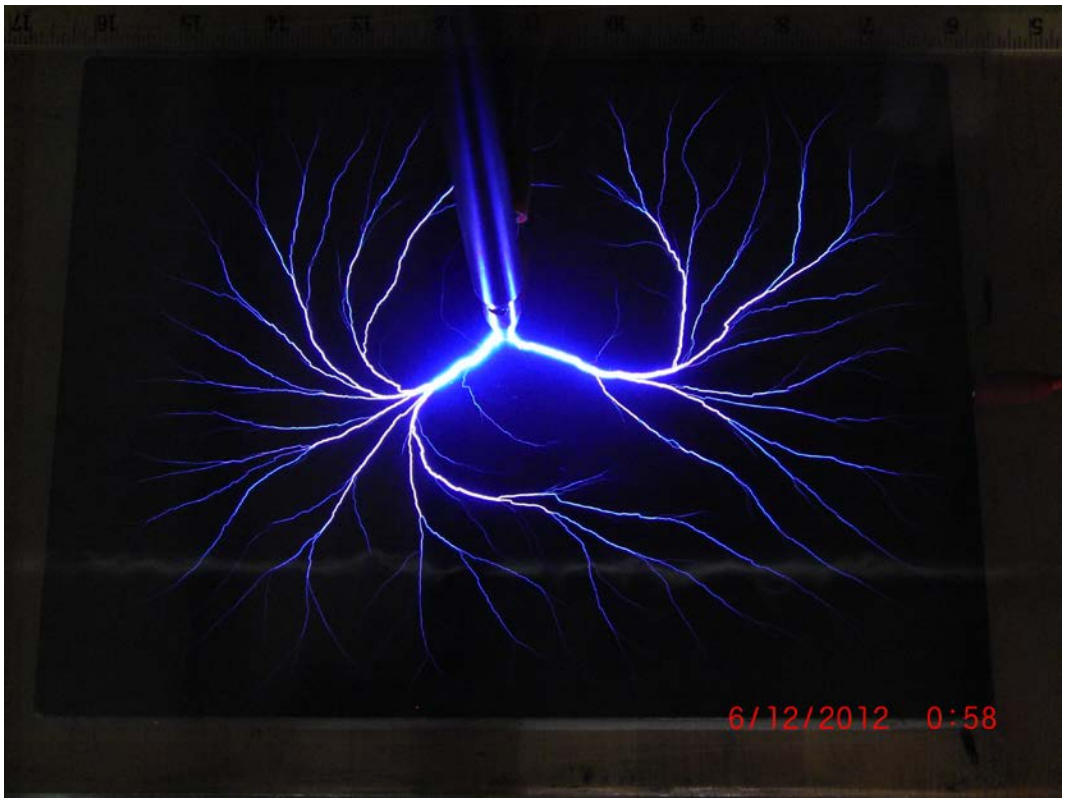

Figure 32: Photograph of a discharge of a stack of three charged Lichtenberg electrets. A 0.5 cm diameter discharge probe was used after each sheet was charged for 5 sec/side and placed in series on the 27.31 cm x 24.13 cm aluminum backplane.

In trying to find applications for the Lichtenberg electret, I placed various light bulbs in series with the discharge rod. The Lichtenberg electret that was charged for ten seconds per side was successful in lighting #222 and #47 flashlight bulbs, which means the current released was able to heat up the filament of the bulb long enough to reach over 2000 K to cause the tungsten filament to glow for a moment. Each of these flashlight bulbs had a power rating of 1W or less, a current rating under 250 mA, and a voltage rating of 2 and 6 V, respectively. A flashbulb used in older model cameras was then hooked up to the system and a successful discharge was obtained with a Lichtenberg electret that was charged for five seconds per side. When a 25 W, 120 V bulb was connected in series with the Lichtenberg electret, the discharge was unable to light the bulb no matter how much the Lichtenberg electret was charged.

Discussions and Conclusions

In conclusion, it was found that through the method of using dielectric barrier discharges as a way to deposit a large amount of stored charge onto the surface of a thin dielectric film, one could create a Lichtenberg electret that can be discharged in a separate location from where it was initially charged. It was found that not all dielectric materials will work to produce the images presented in this study, and the thickness of the material plays a large part in whether the material would work. A number of high-voltage power sources can be utilized to supply the needed corona to charge the surface of the dielectric material including a Ruhmkorff coil and solid-state pulsed DC induction coil power supply. During discharge, only positive figures are created due to charge transfer processes similar to those that describe the creation of lightning strikes between clouds and the ground during lightning storms.

When charging the dielectric sheets, the limit to how much charge that can be stored on the sheet and how strong the coronal discharge can be that deposits the charge is governed by the relative permittivity of the dielectric material. Using a Michelson-Morley interferometer setup, the relative permittivity of the transparency film was determined to be 3.02 ± 0.30. The strength of the coronal discharge would burn right through the thin dielectric sheet causing partial, but significant, discharges that reduces the storage capacity of the sheet if the charging probes were separated by a distance that produced a coronal discharge larger than the dielectric strength of the material. For the transparency film used in this experiment, a separation greater than 5 cm produced coronal discharges that produced electric field strengths greater than the dielectric strength, burning holes in the material. Needlepoint charging probes were chosen because

the maximum amount of charge can be deposited onto the surface of the sheet when the radius of curvature of the probe is the smallest. It was found that more charge could be deposited onto the surface of the sheet when each power supply terminal had multiple needlepoint probes attached to each output because more surface area could be covered in less time.

For a single sheet of transparency film, the current, voltage, and energy released in a given discharge were determined by taking photographs of each discharge using a camera and a current transformer attached to an oscilloscope. The voltage that is typically present during a Lichtenberg discharge is 1.7 MV with a peak discharge current around 13.4 A. This amounts to a release of 0.49 J of energy in approximately 1.24 μs producing a brilliant bluish-white, branching discharge that covers an area of over 500 cm^2 using a 0.5 cm diameter discharge probe attached to an ungrounded aluminum backplane. If a discharge probe of a larger radius of curvature is used, then the resulting discharge has a larger brush discharge that is seen prior the current pulse and usually a smaller peak current value are observed. In contrast, when a parallel plate capacitor setup using a flat circular metal disk and the dielectric sheet in-between the plates was charged instead of the metal plates directly, it was observed that the peak current and electric potential energy increased by a factor of five.

Edge-on photographs were taken and gridlines were printed onto one surface of each sheet to determine that the discharge occurs on the surface of the dielectric sheet and not within the volume. When a discharge occurs on the side with the gridlines, the patterns produced became distorted as the sparks traveled along the conductive ink that made the gridlines. Photographs taken of discharges with the gridlines on the backside of

the sheet made determining the length of each spark easier to determine. As sheets of charged electrets were stacked, discharges occurred in less time and the potential for higher current values, similar in many respects to capacitors in series, were observed.

Lichtenberg figures are already used to diagnose electrical discharge failures in insulation around high-voltage equipment, in klydonographs that record high-voltage surges on power lines due to lightning strikes, and to diagnose lightning strike victims (Graneau 87; Mceachron 716). Research is being conducted to use Lichtenberg figures formed in solids to create molds for artificial biological systems that have fractal properties like blood vessels and vascular tissue. The research presented here could be used by spacecraft researchers to produce Lichtenberg discharges of comparable size to those that they achieve in space as a way to test their equipment before it is sent into orbit without needing a large vacuum chamber and ion gun. These electrets have some applications that pulsed capacitors are currently used for, like ignition devices. Artistically, the method for creating these large electrets could be utilized in photography and cinematography as sources of lightning strikes without the need for a particle beam accelerator to produce the effect on a large scale.

Further research could be conducted on types of materials that will successfully produce Lichtenberg figures in this type of charging situation. More exploration of probe geometry and how that effects the formation of Lichtenberg figure visually as well as the power released could be continued. Figuring out a better way to estimate the released energy during a discharge would be a worthwhile investment as it is not a trivial thing to measure.

References

American Chemical Society National Historic Chemical Landmarks. Scotch® Transparent Tape, 2007. Web. 6 March 2014. <http://www.acs.org/content/acs/en/education/whatischemistry/landmarks/scotchtape.html>.

Anderson, Phillip C. "Characteristics of Spacecraft Charging in Low Earth Orbit." *Journal of Geophysical Research* 117.A7 (2012): n.p. Web. 1 January 2013.

Celestian, Stan. “Fulgurite.” Photograph. *Earth Science Picture of the Day*. Universities Space Research Association. 26 October 2010. Web. 14 July 2015. <http://epod.usra.edu/blog/2010/10/fulgurite.html>.

Femia, N, L Niemeyer and V Tucci. “Fractal characteristics of electrical discharges: experiments and simulation.” *Journal of Physics D: Applied Physics* 26 (1993): 619-627. *IOP Science.* Web. 3 July 2012.

Graneau, Peter. "Lichtenberg Figures Produced by High-Voltage Discharges in Vacuum." *IEEE Transactions on Electrical Insulation* EI-8.3 (1973): 87-91. *IEEE Explore Digital Library*. Web. 8 March 2012.

IBM Corporation. "Fractal Geometry." IBM100: Icons of Progress, 18 May 2011. Web. 15 February 2014. <http://www-03.ibm.com/ibm/history/ibm100/us/en/icons/fractal/words/>.

Lee, Everett S., and C. M. Foust. "The Measurement of Surge Voltages on Transmission Lines Due to Lightning." *Transactions of the American Institute of Electrical Engineers* XLVI (1927): 339-56. Web. 8 March 2012.

MatWeb — Material Property Data. “SABIC Innovative Plastics Lexan® FR63 Polycarbonate Film, Flame Retardant.” MatWeb, 2011. Web. 16 June 2014. <http://www.matweb.com/search/datasheet.aspx?matguid=1a065389891345248baec14ea4c6a2a8&ckck=1>

Mceachron, K. B. "Measurement of Transients by the Lichtenberg Figures." *Transactions of the American Institute of Electrical Engineers* XLV (1926): 712-720. Web. 8 March 2012.

Mueller, L., K. Feser, R. Pfendtner, and E. Fauser. "Experimental Investigation of Discharges for Charged Plastic or Plastic-coated Materials." *Electrical Insulation and Dielectric Phenomena, 2001 Annual Report* (2001): 110-113. *IEEE Xplore Digital Library*. Web. 10 July 2012.

Niemeyer, L., L. Pietronero and H. J. Wiesmann. “Fractal Dimension of Dielectric Breakdown.” *Physics Review Letters*. 52. 12. (1984): 1033-1036. Web. 7 March 2012.

Officeworld.com. *Laser Printer Transparency Film*; MSDS No. 11-5518-3 [Online]. 3M Center: St. Paul, MN, 10 December 1998. Web. 4 February 2014. <http://www.officeworld.com/msds/MMMCG3300.pdf>.

Perger, Warren F. “Using a Michelson Interferometer to Find the Index of Refraction of Materials.” *Michigan Technological University Department of Electrical and Computer Engineering*. EE4441, n.d. Web. 7 February 2014. <http://www.ece.mtu.edu/faculty/wfp/classes/ee4441/Michelson_2.pdf>

Power Electronic Measurements Ltd. “Application Notes.” n.p. 17 August 2002. Web. 23 March 2015. <http://www.pemuk.com/Userfiles/CWT/CWT%20-

%20Technical%20notes%20-%20001.pdf>

Reed, Alan. “Capacitors 1, Fields Revision from A-level Physics Tutor, Your Free Guide for Effective Physics Revision." *A-level Physics Tutor* (2011). Web. 4 February 2014. <http://www.a-levelphysicstutor.com/field-capacit-1.php>.

“Scotch® 311 Box Sealing Tape, 2” x 110 Yd. Product Details.” OfficeDepot. OfficeDepot, n.d. Web. 6 March 2014. <http://www.officedepot.com/a/products/737097/Scotch-311-Box-Sealing-Tape-2/>.

“Scotch® 3750 Commercial Performance Packaging Tape 1 ⅞” x 54.6 Yd., Clear, Pack of 6. Product Details.” *OfficeDepot*. OfficeDepot, n.d. Web. 6 March 2014. <http://www.officedepot.com/a/products/427261/Scotch-3750-Commercial-Performance-Packaging-Tape/>.

Smith, Warren. “Charging a Lichtenberg Electret.” Photograph. *University of Michigan Physics Demonstration Laboratory*. 29 August 2012.

Smith, Warren. “Discharge and Measurement of a Lichtenberg Surface Charged Electret.” Photograph. *University of Michigan Physics Demonstration Laboratory*. 29 August 2012.

Stack, G. E. “Definite-Time Devices Used in Connection with Industrial Control Equipment.” *General Electric Review*. 30, 3. (1927) *IEEE Explore Digital Library*. Web. 12 March 2012

Stoneridge Engineering. "What Are Lichtenberg Figures, and How Are They Made?" n.p. 20 June 2012. Web. 24 July 2012. <http://www.capturedlightning.com/frames/lichtenbergs.html>.

Takahashi, Yuzo. "Two Hundred Years of Lichtenberg Figures." *Journal of Electrostatics* 6.1 (1979): 1-13. Web. 15 March 2012.

ThatScienceGuy. "PreCambrian ProtoHuman." Photograph. *Tumblr.com*. 30 May 2013. Web. 4 February 2014. <http://trilobitesarealive.tumblr.com/>

Thomas, A. Morris. "'Heat Developed' and 'powder' Lichtenberg Figures and the Ionization of Dielectric Surfaces Produced by Electrical Impulses." *British Journal of Applied Physics* 2.4 (1951): 98-109. *IOP Science*. Web. 3 July 2012.

TwistedSifter. "Lichtenberg Figures: The Fractal Patterns of Lightning Strike Scars." Photograph. 10 Mar 2012. Web. 30 May 2013. <http://twistedsifter.com/2012/03/lichtenberg-figures-lightning-strike-scars/>.

Ward, D.A., J. La, and T. Exon. "Using Rogowski Coils for Transient Current Measurements." *Engineering Science and Education Journal* 2.3 (1993): 105-113. Web. 15 March 2012.

Weast, Robert C. *CRC Handbook of Chemistry and Physics*. Boca Raton, FL: CRC, 1990. E-50. Print.

Zeleny, John. "Variations of Size and Charge of Positivie Lichtenberg Figures with Voltage." *American Journal of Physics.* 13 (1945): 106-109. Web. 31 August 2012.